

Chapter 5

Do Radioisotope Clocks Need Repair? Testing the Assumptions of Isochron Dating Using K-Ar, Rb-Sr, Sm-Nd, and Pb-Pb Isotopes

Steven A. Austin, Ph.D.*

Abstract. The assumptions of conventional whole-rock and mineral isochron radioisotope dating were tested using a suite of radioisotopes from two Precambrian rocks. Amphibolite from the Beartooth Mountains of Wyoming shows evidence of thorough metamorphism by isochemical processes from andesite by an early Precambrian magma-intrusion event. A diabase sill, exposed within the wall of Grand Canyon at Bass Rapids, formed by a rapid intrusion event. The event segregated minerals gravitationally, apparently starting from an isotopically homogeneous magma. Although K-Ar, Rb-Sr, Sm-Nd, and Pb-Pb methods ought to yield concordant isochron dates for each of these magmatic events, these four radioisotope pairs gave significantly discordant ages. Special allowance was made for larger-than-conventional uncertainties expressed as 2σ errors associated with the calculated “ages.” Within a single Beartooth amphibolite sample, three discordant mineral isochron “ages” range from 2515 ± 110 Ma (Rb-Sr mineral isochron) to 2886 ± 190 Ma (Sm-Nd mineral isochron). The diabase sill in Grand Canyon displays discordant isochron “ages” ranging from 841.5 ± 164 Ma (K-Ar whole-rock isochron) to 1379 ± 140 Ma (Sm-Nd mineral isochron). Although significant discordance exists between the K-Ar, Rb-Sr, Sm-Nd, and Pb-Pb radioisotope methods, each radioisotope pair appears to yield concordant “ages” internally between whole-rocks and minerals. Internal concordance is best illustrated from the Bass Rapids diabase sill by the tightly constrained Rb-Sr whole-rock and mineral

* *Chairman, Geology Department, Institute for Creation Research, Santee, California*

isochron “ages” of 1055 ± 46 Ma and 1060 ± 24 Ma, respectively. The most problematic discordance is the Sm-Nd and Pb-Pb whole-rock and mineral isochron “ages” that significantly exceed the robust Rb-Sr whole-rock and mineral isochron “ages.” It could be argued that the robust Rb-Sr whole-rock and mineral isochron “ages” are in error, but an adequate explanation for the error has not been offered. The geological context of these Precambrian rocks places severe limitations on possible explanations for isochron discordance. Inheritance of minerals, slow cooling, and post-magmatic loss of daughter radioisotopes are not supported as processes causing isochron discordance in Beartooth amphibolite or Bass Rapids diabase. Recently, geochronologists researching the Great Dyke, a Precambrian layered mafic and ultramafic intrusion of Zimbabwe in southeast Africa, have documented a similar pattern of radioisotope discordance. Alpha-emitting radioisotopes (^{147}Sm , ^{235}U , and ^{238}U) give older “ages” than β -emitting radioisotopes (^{87}Rb and ^{40}K) when applied to the same rocks. Therefore, it can be argued that a change in radioisotope decay rates in the past could account for these discordant isochron “ages” for the same geologic event. Conventional radioisotope clocks need repair.

1. Introduction

Do conventional radioisotope dating methods when applied to a single rock or rock unit give concordant ages? Specifically, do the K-Ar, Rb-Sr, Sm-Nd, and Pb-Pb radioisotope pairs each give the same age, within the uncertainties allowed using radioisotope dating, for a single rock or rock unit? If *concordant* ages were obtained for a single rock or cogenetic suite of rocks using different radioisotope pairs, these would be impressive evidence for the consistency of radioisotope dating and be an affirmation of the assumptions underlying these dating methods. However, if *discordant* ages were obtained, then some qualifications would need to be applied to the assumptions undergirding these dating methods.

We sought to apply the whole-rock and mineral isochron dating methods to answer our question concerning concordant/discordant ages using K-Ar, Rb-Sr, Sm-Nd, and Pb-Pb radioisotope pairs. Specifically, we sought to date ancient rocks that have been in existence through a

major portion of earth history, whose parent isotopes (^{40}K , ^{87}Rb , ^{147}Sm , ^{238}U , ^{235}U , and ^{232}Th) should have been altered by significant amounts of decay to produce significant quantities of daughter isotopes (^{40}Ar , ^{87}Sr , ^{143}Nd , ^{206}Pb , ^{207}Pb , and ^{208}Pb respectively). We sought to date rocks whose geological context is already well understood so that possible geological reasons for isochron discordance could be recognized.

The rationale for the proposed research [Austin, 2000] was to address the kind of discordance obtained from the whole-rock and mineral isochron methods applied to the same rock or cogenetic rock unit. Austin [2000] described the scientific literature concerning multiple dating methods applied to the same rocks. As noted by Austin [2000], discordance of isochron ages is often obtained. Because isochron discordance has not been thoroughly described and explained, Austin [2000] proposed a fourfold classification of isochron discordance:

Category one discordance—a cogenetic suite of rocks with two or more discordant whole-rock isochron ages,

Category two discordance—a cogenetic suite of rocks that generates a whole-rock isochron age older than the associated mineral isochron ages from specific rocks,

Category three discordance—two or more discordant mineral isochron ages from the same rock, and,

Category four discordance—a cogenetic suite of rocks that generates a whole-rock isochron age younger than the associated mineral isochron ages.

Literature review indicates that geochronologists have offered various, sometimes contradictory, and extremely controversial explanations when isochron discordance is obtained for different radioisotope pairs [Austin, 2000]. Category four discordance, where one radioisotope pair gives a whole-rock “age” significantly younger than a mineral isochron “age” of a different radioisotope pair, has been the hardest to explain.

Before we can compare isochron “ages” obtained from different radioisotope pairs, we need a working definition of “concordance” and “discordance.” The age interpretation of an isochron is usually stated in statistical terms derived from the analytical precision of the points defining the line on an isochron plot. As Ludwig [2001] noted in a

hypothetical example of a particular formation being dated, if we find eight points whose regression gives an isochron age of 320 ± 8 Ma (2σ), then this result is equivalent to the statement:

If one were to repeat the sampling and regression procedure an infinite number of times, the probability that the grand mean of the resulting isochron ages would fall between 312 and 328 Ma is 95%.

Ludwig, [2001] noted,

... this statement does not say that the *true* age of the samples has a 95% probability of falling between 312–328 Ma, only that the mean of the infinitely-replicated regressions would yield an isochron age within this interval.

As affirmed by Ludwig, three other factors also affect the real age uncertainty (not the conventional “analytical-error-only” uncertainty) associated with isochrons:

- (1) errors concerning the assumption of a closed system,
- (2) errors concerning the invariant beginning isotope ratio, and
- (3) errors concerning the parent radioisotope decay constant.

Renne *et al.* [1998] affirmed in the title of their paper, “Absolute ages aren’t exactly” because these age determinations usually fail to incorporate uncertainties associated with the modern measurements of decay constants. Thus, at least *four* uncertainties must be incorporated into our understanding of the overall error associated with any isochron. The real uncertainty may be significantly larger than the commonly stated “analytical-error-only” uncertainty.

A special case involving the massive volcanism in the Siberian Traps at the Permian-Triassic boundary illustrates our need for a rigorous definition of isochron concordance and discordance. Renne *et al.* [1998] reported for Siberian volcanism a high-precision ^{238}U - ^{206}Pb date of 251.3 ± 0.2 Ma and a high-precision $^{40}\text{Ar}/^{39}\text{Ar}$ date of 250.0 ± 0.3 Ma. These two dates assume 2σ errors derived only from uncertainties in the analytical methods. The two dates appear to be *discordant*. However, as recognized by Renne *et al.* [1998], significant error exists in both our estimate of the ^{40}K decay constant and in the isotope ratio of standards used to calibrate the $^{40}\text{Ar}/^{39}\text{Ar}$ method. Thus, a better expression of the $^{40}\text{Ar}/^{39}\text{Ar}$ date, according to Renee *et al.* [1998], is 250.0 ± 4.4 Ma, clearly

not statistically resolvable from the ^{238}U - ^{206}Pb date of 251.3 ± 0.2 Ma. Therefore, these two ages by the two radioisotope pairs can be regarded as *concordant*.

Recently, the geochronologic community has recommended a new method for evaluating uncertainties associated with isochron ages [Ludwig, 2001]. A statistic called the “mean square of weighted deviates” (MSWD) is a ratio characterizing the observed scatter of the points (from the best-fit regression line of an isochron) to the expected scatter (from the various assigned errors, including but not limited to, analysis equipment). If the assigned errors have been correctly characterized, the observed scatter should approximate the expected scatter, so the value of MSWD should be near unity. Thus, two isochrons having errors assigned to points both giving MSWD values near unity will express two uncertainties associated with the two calculated “ages” that will be better suited to evaluate “concordance” than the older method of using “analytical-error-only” uncertainties. Therefore, “concordance” between two isochron ages must incorporate this expanded understanding of isochron uncertainties.

For data contained in this paper we attempt to incorporate broader estimates of isochron errors. When we quote isochron determinations of other scientists, we use care to define which uncertainties these scientists are using.

Two Precambrian rock units were selected for detailed radioisotope analysis in this study. The purpose was to recognize, classify, and evaluate isochron concordance/discordance within specific rocks and within cogenetic units of rocks by the K-Ar, Rb-Sr, Sm-Nd, and Pb-Pb radioisotope pairs. The first rock unit selected is a lower Precambrian (Archean) metamorphic rock from the southeastern Beartooth Mountains of Wyoming (Figure 1). The second rock unit is the upper Precambrian (Proterozoic) diabase sill at Bass Rapids in the central Grand Canyon, Arizona (Figure 2).

2. Geologic Setting of the Beartooth Amphibolite

Ancient metamorphosed basement rocks comprise the deeper

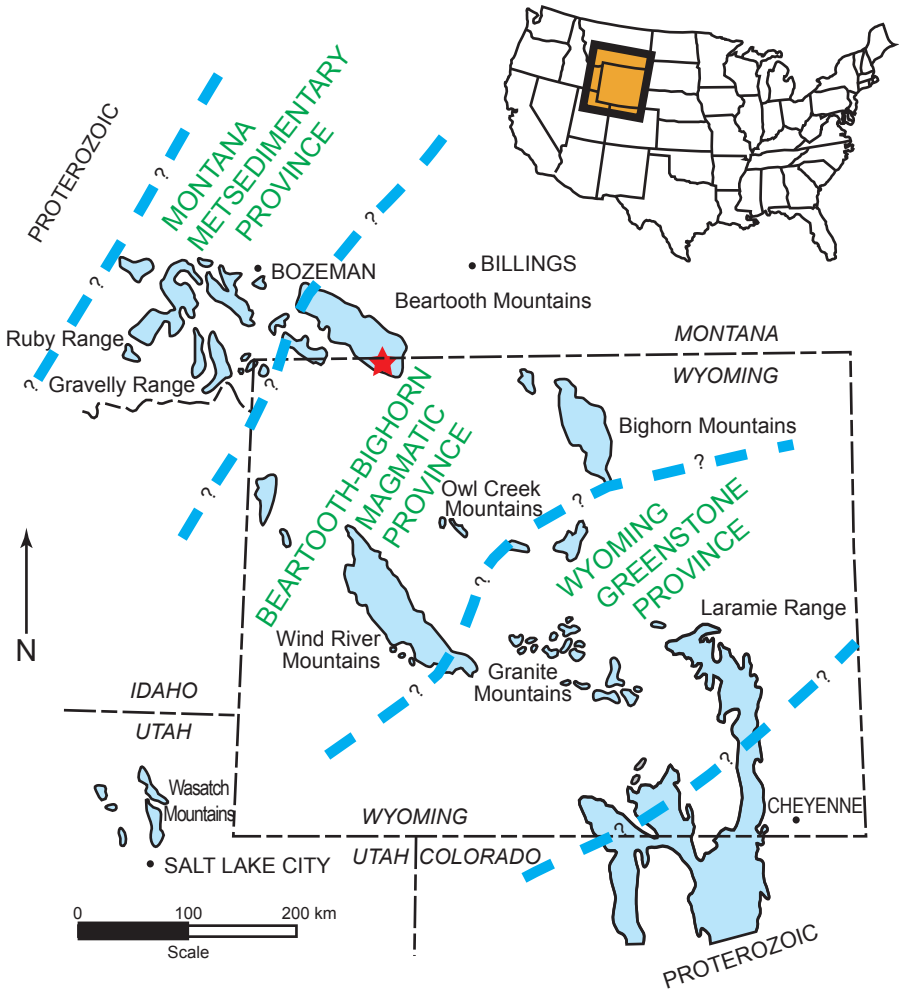


Figure 1. Location map showing the distribution of Precambrian rocks in the northern Rocky Mountain region. The map shows the location of the Beartooth Mountains and the collection site of Beartooth andesitic amphibolite sample BT-1 (indicated by ★ in northwestern Wyoming). Three provinces of Archean rocks in Montana and Wyoming are positioned between two regions of younger Proterozoic rocks (after *Mueller et al.* [1998]).

continental crust in the northern Rocky Mountain region of the United States. Tectonic and erosion processes have exposed these basement

rocks within numerous mountain ranges (Figure 1). According to *Mueller et al.* [1998], the Archean rocks of this region can be divided into three southwest-to-northeast-trending belts or provinces: the Montana metasedimentary province (Idaho and western Montana), the Beartooth-Bighorn magmatic province (northwestern Wyoming and eastern Montana), and the Wyoming greenstone province (southeastern Wyoming). These three Archean metamorphic provinces are sandwiched between younger Proterozoic rocks on the northwest and southeast (Figure 1).

Gneissic rocks within the core of the Beartooth Mountains of northwestern Wyoming and south-central Montana lie within the Beartooth-Bighorn magmatic province (Figure 1). Archean rocks of the Beartooth Mountains are widely claimed to be among the oldest rocks within the United States dating to about 3000 Ma [*Mueller et al.*, 1987, 1998]. Granitic rocks within the mountains have enveloped a wide variety of older rock types; the most common of these is fine- to coarse-grained amphibolite of andesitic composition [*Mueller et al.*, 1983]. Metamorphic rocks of the Beartooth complex also include lesser amounts of mafic amphibolites, quartzite, tonalitic gneiss, granitic gneiss, ironstone and impure quartz-rich rocks [*Mueller et al.*, 1987].

The most carefully studied andesitic amphibolite comes from the Long Lake magmatic complex on the Beartooth Highway in Wyoming [*Mueller et al.*, 1988]. According to *Warner et al.* [1982], this complex includes andesitic amphibolite intruded by Long Lake granodiorite (foliated granitic to tonalitic rocks) and Long Lake granite (more massive leucocratic granite to tonalite). Metasedimentary inclusions of orthoquartzite include detrital zircons dated up to 3960 Ma [*Mueller et al.*, 1998]. Using major and trace elements, particularly the light rare earth elements, *Mueller et al.* [1983] argued that the elemental abundance pattern of the andesitic amphibolite is the result of an isochemical metamorphic process with final crystallization reactions associated with the intrusion of Long Lake granodiorite and granite. According to *Mueller et al.* [1983], granitic intrusions did not significantly alter the original chemistry of the andesitic amphibolite. Mineral assemblages within the amphibolite indicate that original igneous rocks were

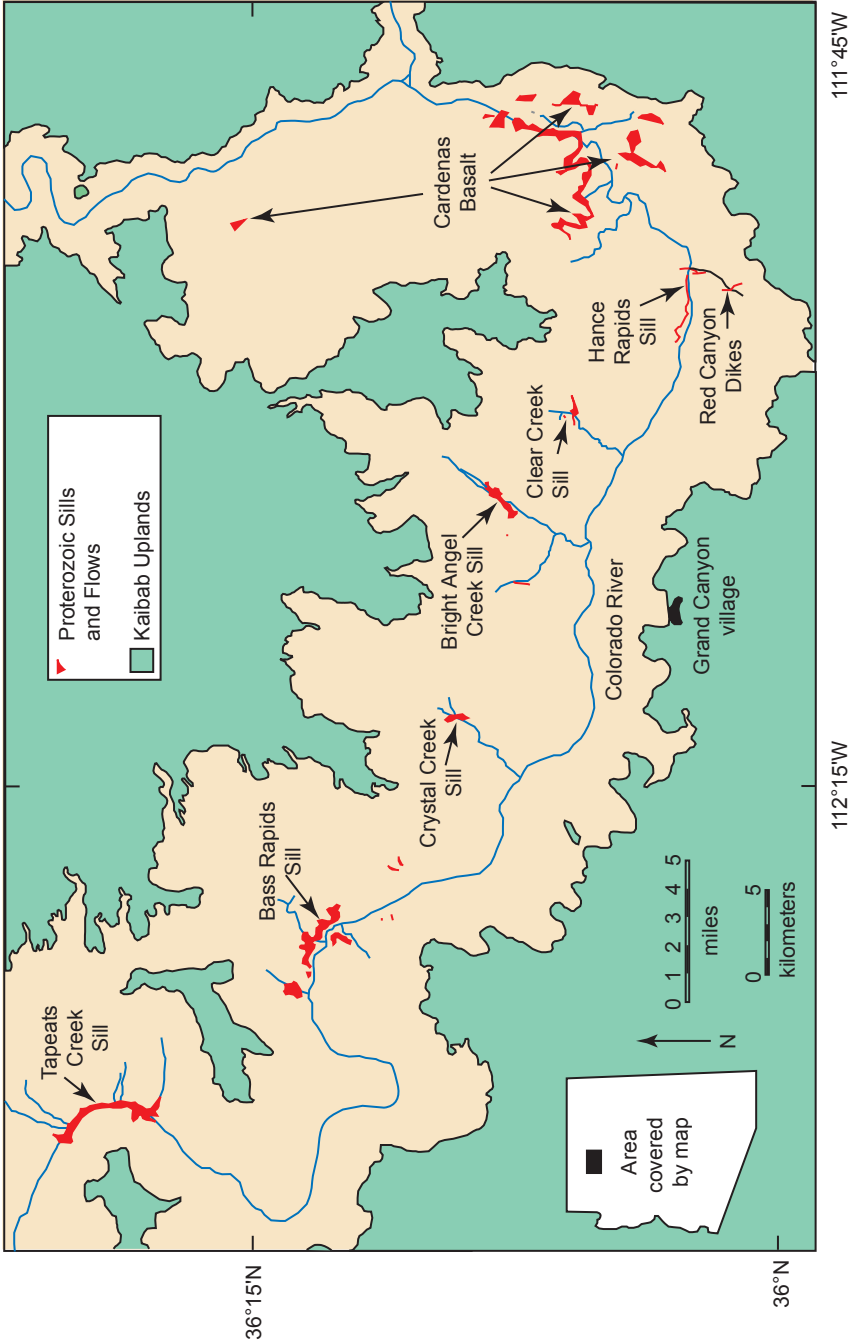


Figure 2. Location of the Bass Rapids diabase sill in Grand Canyon, northern Arizona.

metamorphosed to the epidote-amphibolite facies at a final equilibration temperature of about 400°C [Warner *et al.*, 1982]. Geochemistry and mineralogy do not support hydrothermal metasomatism. According to Mueller *et al.* [1983], the amphibolites were derived from andesite, specifically an andesite enriched in rare earth elements and other incompatible trace elements. Beartooth amphibolites are dominated by plagioclase, quartz, hornblende, and biotite, with lesser amounts of magnetite, ilmenite and titanite. Biotite strongly fractionates Rb at the expense of Sr, and titanite strongly fractionates rare earth elements (for example, Sm), as well as U and Th. Thus, because significant variation in parent radioisotope abundance is required for isochron dating, whole-rock and mineral isochron methods should be able to discern the age of the amphibolite.

Significant effort has been expended to date Beartooth rocks. A 2790 Ma model date was obtained by U-Pb in a zircon from the andesitic amphibolite [Mueller *et al.*, 1987]. This age was confirmed by an impressive, 28-point Rb-Sr whole-rock isochron age of 2790±35 Ma (initial $^{87}\text{Sr}/^{86}\text{Sr} = 0.7022 \pm 0.0002$ and uncertainties from analytical errors being 2σ). Figure 3 shows this whole-rock isochron replotted from the data of Wooden *et al.* [1982], including thirteen samples of Long Lake granite (plotting mostly in the more-radiogenic area in the upper right), five samples of Long Lake granodiorite (plotting mostly near the middle), and ten samples of amphibolite (plotting in the lower left). The 2790 Ma isochron is supposed to date the thermal event that recrystallized and homogenized the Sr isotopes of these metamorphic rocks [Wooden *et al.*, 1982]. The granitoid rocks of the southeastern Beartooth Mountains gave a Rb-Sr whole-rock isochron age of 2810±40 Ma with initial $^{87}\text{Sr}/^{86}\text{Sr} = 0.7018 \pm 0.0002$, an age and initial Sr ratio essentially indistinguishable from the amphibolite [Mueller *et al.*, 1983]. The protolith from which the andesitic amphibolite recrystallized is suggested to be 2950 Ma [Mueller *et al.*, 1983].

3. Geologic Setting of the Bass Rapids Diabase Sill

Mafic igneous rocks occur as sills, dikes and flows in the thick

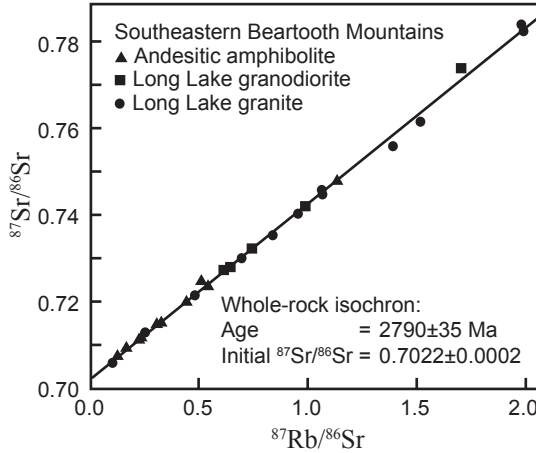


Figure 3. Composite Rb-Sr whole-rock isochron from the Long Lake granitic complex in the southeastern Beartooth Mountains of northwestern Wyoming. Plot includes Long Lake granite (thirteen samples), Long Lake granodiorite (five samples), and Beartooth andesitic amphibolite (ten samples). Data replotted from *Wooden et al.* [1982].

succession of strata making up the middle Proterozoic Unkar Group of the Grand Canyon, Arizona (Figure 2). The Unkar Group sedimentary sequence is comprised of four formations (in ascending order, the Bass Limestone, Hakatai Shale, Shinumo Quartzite and the Dox Sandstone) which are overlain by the 300 m plus thick flow sequence of lava flows of the Cardenas Basalt [*Hendricks and Stevenson, 1990, 2003*]. The younger Precambrian sediments of the Nankoweap Formation and the Chuar Group overlie this Unkar Group succession, which unconformably rests on the early Proterozoic metamorphic and igneous crystalline basement [*Babcock, 1990; Ilg et al., 1996; Karlstrom et al., 2003*].

The diabase sills and dikes are believed to be the intrusive equivalents of the Cardenas lava flows, but they are not found in direct association with the Cardenas Basalt [*Hendricks, 1972, 1989; Hendricks and Lucchitta, 1974*]. Thus the relationship between them is obscure because the direct feeders to the flows have never been recognized among the available diabase outcrops. The diabase sills are, in fact, confined to

the lower part of the Unkar Group, particularly intruding near the boundary between the Bass Limestone and Hakatai Shale, whereas the related dikes are intruded into all the formations above the sills along faults that predate, or are contemporaneous with, the sills. These mafic sills crop out in seven locations along a 70–80 km length of the Grand Canyon (Figure 2), whereas the Cardenas Basalt flows are restricted to the area around Basalt Canyon in the eastern Grand Canyon. The sills range in thickness from 20 m (about 65 feet) near Hance Rapids in the east to more than 200 m (655 feet) near Tapeats Creek in the west. They are composed chiefly of medium-grained ophitic olivine-rich diabase that is uniform in texture and mineralogy from sill to sill in the Canyon. The dikes have a similar composition but are finer grained, as are the chilled margins of the sills. Early in-place differentiation and crystal settling in the sills is evidenced by granophyre layers up to 6 m thick and felsite dikes, and by layers that are richer in olivine.

Noble was the first to describe the diabase sills in the Bass Canyon-Shinumo Creek area [Noble 1910, 1914]. Maxson [1967, 1968] mapped the intrusive rocks of the Grand Canyon but did not describe the diabase sills and dikes. Detailed mapping and sampling of the sills and dikes, and the Cardenas Basalt flows, followed by petrographic examination and chemical analysis of the samples collected, were reported by Hendricks [1972, 1989] and Hendricks and Lucchitta [1974]. They found that chemical variation diagrams indicated a potential common parentage for the diabase in the sills and the lower third of the basalt flows. However, the flows in the upper two-thirds of the Cardenas Basalt sequence were found to be much more silicic than the diabase sills, and, therefore, it was concluded that they probably were not emplaced during the same phase of igneous activity. Nevertheless, the mineral composition of the unaltered basalt flows in the bottom third of the sequence is similar to that of the diabase sills, which suggested that those lavas and the diabase sills were co-magmatic and probably coeval. Thus, they concluded that the basalt lavas in the top two-thirds of the sequence were extruded after differentiation of the parent magma.

The 1.1 Ga Rb-Sr isochron date for the Cardenas Basalt is widely regarded as perhaps the best “age” obtained for Grand Canyon strata

[*McKee and Noble, 1974; Larson et al, 1994*]. This date was derived from two whole-rock Rb-Sr data sets combined to form a ten-point isochron plot. According to *Larson et al. [1994]*, the Rb-Sr whole-rock isochron age of the Cardenas Basalt based on two data sets (ten points) is 1103 ± 66 Ma (uncertainty assumes 2σ analytical errors) with initial $^{87}\text{Sr}/^{86}\text{Sr}$ of 0.7062 ± 0.0024 (again, uncertainty assumes 2σ analytical errors). This age and the initial Sr ratio are statistically indistinguishable from 1070 ± 70 Ma and $^{87}\text{Sr}/^{86}\text{Sr}$ of 0.7065 ± 0.0015 (2σ analytical errors with age recalculated using new ^{87}Rb decay constant) originally obtained from the five-point isochron by *McKee and Noble [1974]* and restated by *McKee and Noble [1976]*. According to *Elston and McKee [1982]*, the Bass Rapids diabase sill yields a five-point Rb-Sr whole-rock isochron age of 1070 ± 30 Ma and initial $^{87}\text{Sr}/^{86}\text{Sr}$ of 0.7042 ± 0.0007 (2σ analytic errors). This age for the Bass Rapids diabase sill provided apparent confirmation of the relationship between the diabase sills and the Cardenas Basalt flows, and this age appears to have less uncertainty than the age of the associated Cardenas Basalt. Figure 4 shows the Bass Rapids diabase sill Rb-Sr whole-rock isochron originally published by *Elston and McKee [1982; their Figure 7]*. The higher precision of age and initial Sr of the Bass Rapids diabase sill [*Elston and McKee, 1982*] comes from the wider spread in the Rb-Sr data on the isochron plot because two of the data points are from high-Rb granophyre occurring at the top of the sill. As shown by *Elston and McKee [1982]*, the Bass Rapids diabase sill provides every indication that it was well mixed isotopically when it was intruded, even though during cooling the sill segregated mineralogically and chemically by crystal settling to produce a granophyre on top of the diabase. Such a condition of initial thorough isotopic mixing of the original magma body followed by rapid chemical segregation is suited to the assumptions of whole-rock and mineral isochron dating.

Hendricks and Stevenson [1990, 2003] have summarized most of the details of the Unkar Group, including the diabase sills and dikes, and the Cardenas Basalt flows. Subsequently, while focusing on the Cardenas Basalt, *Larson et al. [1994]* found that, whereas the major-element chemistry of the diabase sills exhibit similarities and dissimilarities

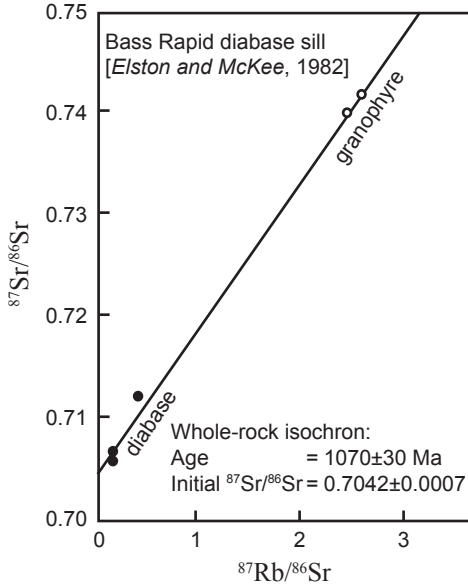


Figure 4. The original Rb-Sr whole-rock isochron plot for the Bass Rapids diabase sill published by *Elston and McKee* [1982]. Isochron age obtained was 1070 ± 30 Ma.

with the lower-member flows of the Cardenas Basalt [*Hendricks and Lucchitta, 1974*], the trace and rare earth element data from a sample of the sill at Hance Rapids show very similar variation patterns to those in the lower-member flows of the Cardenas Basalt. Only Ti and P contents are markedly higher in the sill, and the negative Eu anomaly for the sill is smaller than that for the lower-member Cardenas Basalt flows. Thus, *Larson et al.* [1994] suggested a common origin for the diabase of the sills and the basalt of the lower-member flows similar to continental flood basalts, except that the higher Ti and P contents of the diabase may indicate that the magma that fed the intrusions did not also directly feed the flows of the lower member. Alternately, they suggested that the higher silica, Ti and P contents of the basalt flows are due either to greater crustal contamination of the basalt magma on its passage to the earth's surface, or heterogeneity in the mantle source. Paleomagnetic

determinations by *Elston and Grommé* [1974], *Elston and McKee* [1982], and *Elston* [1989] suggested that the diabase sills have a different paleomagnetic pole position than the Cardenas Basalt flows. *Elston and McKee* [1982], recognizing the analytical uncertainties of the Rb-Sr measurements, suggested that the sills date 40–50 Ma older than the Cardenas Basalt. However, *Weil et al.* [2003] argued that the sills and associated Cardenas Basalt have the same paleomagnetic pole position, and could, therefore, be the same age. Although the Rb-Sr whole-rock isochron ages are identical for the Cardenas Basalt and the Bass Rapids diabase sill, the flows and sill were found to have slightly different initial $^{87}\text{Sr}/^{86}\text{Sr}$ ratios (see above, 0.70650 ± 0.0015 and 0.70420 ± 0.0007 , analytical errors 2σ respectively). This small initial Sr difference is probably due to bias in sampling the Cardenas Basalt. Bias was introduced because *Elston and McKee* [1982] did not sample the lower flows of the Cardenas Basalt that are lower in radiogenic Sr.

Potassium-Ar analysis of Precambrian diabase and Cardenas Basalt of Grand Canyon has not presented ages concordant with Rb-Sr. A K-Ar model age of 944 Ma was obtained on pyroxene extracted from a sample of the diabase sill, presumably at Hance Rapids, by *Ford et al.* [1972], whereas *Elston and McKee* [1982] obtained two K-Ar model ages of 913 ± 40 Ma for pyroxene in the diabase sill at Hance Rapids, and 954 ± 30 Ma for plagioclase from the diabase sill at Tapeats Creek (K-Ar model ages are reported here, as is customary in the literature, with 1σ analytical errors). Additionally, *Elston and McKee* [1982] reported a total fusion $^{40}\text{Ar}/^{39}\text{Ar}$ age of 907 ± 35 Ma for pyroxene from the diabase sill near Shinumo Creek and a $^{40}\text{Ar}/^{39}\text{Ar}$ isochron age of 904 ± 100 Ma from seven-step incremental heating of a whole-rock sample from the diabase sill at Tapeats Creek. *Austin and Snelling* [1998] reported K-Ar data on five further samples of these Grand Canyon intrusive rocks, one from the diabase dike in Red Canyon adjacent to Hance Rapids, one from the diabase sill near Hance Rapids, and three from the sill near Bass Rapids (one diabase and two granophyre). The K-Ar model ages range from 703 ± 15 Ma to 895 ± 20 Ma. When combined with the two samples analyzed by *Elston and McKee* [1982], the K-Ar data yield a K-Ar seven-point isochron. According to *Austin and Snelling* [1998] the

K-Ar whole-rock isochron age of the Grand Canyon diabase intrusives is 837 ± 52 Ma, significantly discordant with *Elston and McKee's* [1982] Rb-Sr five-point isochron age of 1070 ± 30 Ma for Bass Rapids diabase sill (both isochron ages with 2σ analytical uncertainties). *Larson et al.* [1994] argued that the post-emplacement cooling temperatures of the Cardenas Basalt and diabase intrusives never exceeded 250°C and a pressure of 1.5 kbar. They supposed that Ar leakage might explain the anomalously young K-Ar ages. *Timmons et al.* [2001] reported $^{40}\text{Ar}/^{39}\text{Ar}$ spectra ages for three diabase intrusives that are consistent with the K-Ar model ages. *Timmons et al.* [2001] supposed that a hydrothermal event at about 800 Ma caused pervasive Ar leakage. *Austin and Snelling* [1998] noted the systematic ^{40}Ar variation in Cardenas Basalt and diabase sills is not matched by a systematic loss pattern for non-radiogenic ^{36}Ar . They concluded that the Rb-Sr and K-Ar discordance could not be explained by Ar loss due to either resetting or leakage. *Austin and Snelling* [1998] offered three alternative explanations—

- (1) argon inheritance,
- (2) argon mixing, or
- (3) change in the radioisotopic decay rates that affected ^{87}Rb and ^{40}K decay by different factors.

The sill at Bass Rapids appears to be the best candidate for detailed radioisotopic study. How then are the radioisotope daughters distributed through the granophyre and diabase, and through the mineral phases of the latter? The various radioisotope pairs would be expected to give concordant whole-rock isochron and mineral isochron “ages.” However, published K-Ar model “ages” for the diabase sills (and the Cardenas Basalt) are significantly younger than their associated Rb-Sr isochron “ages” [*Elston and McKee*, 1982; *Austin and Snelling*, 1998].

For this study the thick sill near Bass Rapids was chosen because of its excellent outcrop exposures and because of its well-defined 6 m thick granophyre layer on top of the 85 m thick diabase [*Snelling et al.*, 2003]. Furthermore, more geochemical and radioisotopic analyses have been undertaken previously on this sill than any of the other sills in Grand Canyon.

4. Sample Collection, Preparation and Analysis

4.1 Beartooth Andesitic Amphibolite

A single, multi-kilogram sample of the Beartooth andesitic amphibolite was collected from the southeastern Beartooth Mountains of northwestern Wyoming to see if concordant mineral isochrons could be obtained by K-Ar, Rb-Sr, Sm-Nd, and Pb-Pb. The sample was collected from a road cut on U. S. Highway 212, west of Beartooth Pass, 1.3 km east-northeast of Long Lake (Deep Lake, Wyoming 7.5 minute Quadrangle, U. S. G. S., 1991). The outcrop sampled is on the east side of Highway 212 at North $44^{\circ} 52.187'$ latitude and West $109^{\circ} 28.937'$ longitude (North American Datum of 1927) with a position error estimate by G. P. S. and topographic control of about 10 m. The sample location is an exposure in the deep excavation engineered for the highway at an elevation of 3110 m. The rock possesses excellent coarse-grained crystalline texture with very little evidence of weathering or low-temperature alteration. The outcrop was specifically selected because it was apparently one of the sample locations of *Wooden et al.* [1982] for their Rb-Sr whole-rock isochron. Thus, this andesitic amphibolite was used by *Wooden et al.* [1982] to define the Rb-Sr isochron's slope (and, therefore, the age of the cogenetic suite), as well as to define the assumed initial homogeneous Sr from which the cogenetic suite of rocks is supposed to have evolved. This rock is, therefore, considered representative of the andesitic amphibolite in the southeastern Beartooth Mountains.

The Beartooth andesitic amphibolite sample comes from a tabular amphibolite body that is tens of meters wide. It is in contact association with the Long Lake granodiorite, an intrusive igneous body that is supposed to have metamorphosed the amphibolite [*Wooden et al.*, 1982]. The amphibolite sample possesses coarse-grained, equigranular texture with slight foliation due to the biotite. Grain size is approximately 1 mm. Major mineral composition in order of abundance by weight is plagioclase, quartz, biotite, hornblende, magnetite, and titanite. The amphibolite appears ideal for mineral isochron analysis because biotite, titanite and hornblende fractionate radiogenic parent isotopes.

The Beartooth andesitic amphibolite sample was crushed in an iron mortar to produce 1.01 kg of sieved powder consisting of -140 to +270 mesh grains representative of the whole rock. The powder passed through the 140-mesh sieve (140 squares per inch) but was collected on top of a 270-mesh sieve (270 squares per inch). Five mineral separates from the powders were progressively concentrated by centrifugation in three heavy liquids diluted to produce liquids of precisely calibrated densities. Centrifugation was performed on up to 1 liter bottles of heavy liquids with high-strength armatures delivering g-forces more than 50 times normal gravity. The three heavy liquids used were tribromomethane (CHBr_3) with specific gravity of 2.85 at room temperature, diiodomethane (CH_2I_2) with specific gravity of 3.32 at room temperature, and a solution of thallium malonate-formate [$\text{HCO}_2\text{TlCH}_2(\text{COOTl})_2$] in water with a specific gravity at full saturation of about 4.05 at room temperature. Dilutents used to adjust densities of heavy liquids included acetone, distilled water and ethyl alcohol. Cleaning and concentration using a strong magnet followed heavy-liquid separations. Microscopic examination and x-ray diffraction analyses insured excellent recovery of the desired mineral phases. The five mineral phases separated from the Beartooth amphibolite whole-rock were

- (1) quartz-plagioclase,
- (2) biotite,
- (3) hornblende,
- (4) magnetite, and
- (5) titanite.

Because of the density similarity of quartz and plagioclase, we were unable to separate quartz from andesine. The six samples (whole-rock plus five mineral separates) had abundant grains for K-Ar, Rb-Sr, Sm-Nd and Pb-Pb analyses plus elemental and x-ray diffraction analyses.

4.2 Bass Rapids Diabase Sill

The Bass Rapids diabase sill was sampled as eleven rocks from a

composite section through the sill at Bass Rapids (north bank of the Colorado River at mile 107.6 to 108.0), the same section sampled from outcrop by *Hendricks and Lucchitta* [1974] some 800 m east of Shinumo Creek [*Snelling et al.*, 2003]. The eleven samples were chosen to represent the overall petrographic variability within the complete thickness of the sill (Figure 5). Eight of the samples are diabase from the lower approximately 85 m of the sill. Three of the samples are from the 6 m thick granophyre at the top of the sill. These eleven whole-rock samples were prepared by clean laboratory techniques as -200-mesh powders for chemical and isotopic analyses. Thin-sawed slices of the whole rocks were prepared as thin sections for petrographic analysis. Two of the eight diabase samples representative of the sill were each crushed to produce more than 1 kg of -140 to +270 mesh grains, and the various minerals within the powders were progressively concentrated by centrifugation in the three different heavy liquids, followed by further cleaning using a strong magnet. Six mineral phases were thus separated from whole-rock diabase sample DI-13 (normal plagioclase, high-density plagioclase, biotite, clinopyroxene, olivine and magnetite). Using the experience gained from sample DI-13, a very thorough search was made for smaller quantities of additional mineral phases in whole-rock sample DI-15. Eleven mineral phases were separated from sample DI-15 (plagioclase, high-density plagioclase, biotite, normal clinopyroxene, high-density clinopyroxene, orthopyroxene, normal hornblende, high-density hornblende, olivine, ilmenite, and magnetite). The Fe-Ti oxide (opaque “titanomagnetite” in thin section) of the diabase contains mostly magnetite, but the less-abundant mineral ilmenite occurs as well. In sample DI-15 a small quantity of ilmenite was recovered. Because “titanomagnetite” was so easily separated from these rocks, magnetite (with a small fraction of ilmenite) was separated from samples (DI-7, DI-10, DI-11, DI-16, and DI-17). X-ray diffraction analysis (XRD) and/or optical microscopy were used to confirm the identity and purity of the minerals concentrated.

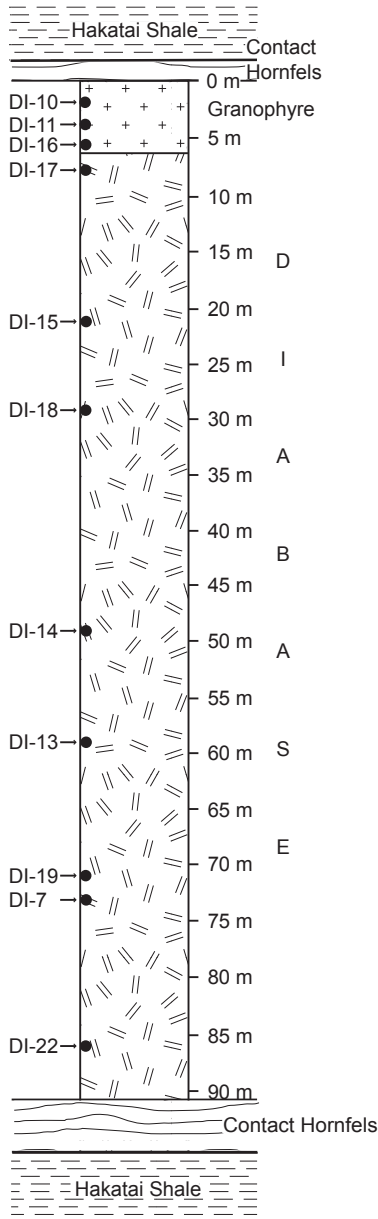


Figure 5. Diagrammatic section through the Bass Rapids sill showing the 6 m thick granophyre capping above the 85 m thick diabase body of the sill. The location of samples within the sill is indicated (after *Snelling et al.* [2003]).

4.3 Analysis Procedures

X-ray diffraction analyses of mineral separates were performed on a Scintag x-ray diffractometer scanning from 5 to 50° 2 θ using a Cu K- α radiation, with the resulting patterns matched to more than 60,000 reference standards in the Joint Committee for Powder Diffraction Standards database. Sam Iyengar was the XRD analyst.

All Beartooth andesitic amphibolite and Bass Rapids diabase sill samples were analyzed for major and trace elements. XRAL Laboratories of Don Mills, Ontario, using XRF (x-ray fluorescence), ICP (inductively coupled plasma), and ICP-MS (inductively coupled plasma mass spectrometer) methods, performed chemical analyses of the whole-rock powders for 67 elements.

Whole rocks were subjected to standard K-Ar analysis by Geochron Laboratories, Cambridge, Massachusetts (R. Reesman, analyst) and Activation Laboratories, Ancaster, Canada (Y. Kapusta, analyst). The abundance of K was measured in whole rocks by flame photometry. Additionally, the five mineral separates from the Beartooth amphibolite, because of their abundance, were submitted as 5 g separates for K-Ar analysis, but technical problems occurred in the acid digestion process of magnetite and titanite. Potassium-Ar data on Beartooth andesitic amphibolite include only four parts, the whole-rock, quartz-andesine, hornblende and biotite.

Rubidium-Sr, Sm-Nd, and Pb-Pb analyses were performed on whole-rocks and mineral separates using a Finnigan-MAT 6-collector solid source mass spectrometer at the University of Colorado. *Farmer et al.* [1991] described the analytic technique, and G. L. Farmer supervised the analysis process. Rubidium, Sr, Sm, Nd, and Pb were separated by conventional cation-exchange chromatography; isotopic concentrations were measured by isotope dilution analysis. The U.S.G.S. andesite AGV-1 standard yielded Rb and Sr concentrations within 1.0% of the accepted value. The CIT mixed Sm/Nd standard yielded Sm and Nd concentrations within 0.7% of the accepted values. The NIST Sr isotopic standard yielded $^{87}\text{Sr}/^{86}\text{Sr}$ of 0.71028 ± 0.0002 (2σ) during the time period of most of the measurements. The La Jolla Nd isotopic

standard yielded $^{143}\text{Nd}/^{144}\text{Nd}$ of 0.511838 ± 0.00005 (2σ) during the time period of most of the measurements. Lead isotope ratios were calibrated relative to NBS-981 with standard deviations (2σ) for $^{206}\text{Pb}/^{204}\text{Pb}$ of 0.19%, $^{207}\text{Pb}/^{204}\text{Pb}$ of 0.2%, and $^{208}\text{Pb}/^{204}\text{Pb}$ of 0.28% during the time of most of the measurements.

Technical problems were encountered in isotope dilution analysis of the abundance of Sm and Nd in the mineral titanite from the Beartooth amphibolite. The extremely high abundance of Sm and Nd in titanite required several attempts to achieve reproducibility of the measurements at the University of Colorado. Two separate splits of titanite were supplied for Sm-Nd analysis with close agreement obtained.

Radiogenic isotope data were interpreted by the popular software package called *Isoplot* written by Kenneth R. Ludwig of the Berkeley Geochronology Center [Ludwig, 2001]. *Isoplot* does basic plotting and calculation functions including the Rb-Sr, Sm-Nd, and Pb-Pb isochrons. The slope of the linear-array plot is interpreted to be an isochron by *Isoplot* using the two-error regression method of York [1969]. *Isoplot* calculates the “mean square of weighted deviates” (MSWD), a ratio of the observed scatter of the points from the best-fit line to the expected scatter from the assigned errors. *Isoplot* also calculates a probability that helps evaluate the degree of confidence one might attach to an isochron.

5. Petrography and Chemistry

5.1 Beartooth Andesitic Amphibolite

The coarse-grained, equigranular, Beartooth andesitic amphibolite displays excellent crystallinity in thin section. Major mineral composition in order of abundance by weight is plagioclase (44%), quartz (27%), biotite (16%), hornblende (7%), magnetite (3%), and titanite (2%). Table 1 displays the major element oxides and abundances of selected trace elements. Biotite, and to a lesser degree hornblende, form the foliated texture of the metamorphic rock. Plagioclase is strongly twinned andesine ($\text{An} \approx 30$ composition) dominating the prominent,

Table 1. Major-element oxide and selected trace element analyses of the Beartooth andesitic amphibolite from the southeastern Beartooth Mountains, northwest Wyoming. Analysis includes the whole-rock BT-1 and five mineral separates. (Analyst: XRAL Laboratories of S.G.S. Canada, Don Mills, Ontario, October 1999.)

Oxide/Element	BT-1WR	BT-1QA	BT-1B	BT-1H	BT-1M	BT-1T
	Whole Rock	Quartz-Andesine	Biotite	Hornblende	Magnetite	Titanite
SiO ₂ (%)	56.9	69.9	38.0	40.4	3.03	28.9
TiO ₂ (%)	1.50	0.34	1.85	1.35	0.45	29.1
Al ₂ O ₃ (%)	13.9	15.4	14.3	11.0	0.71	1.69
Fe ₂ O ₃ (%)	11.1	0.77	19.2	20.6	95.3	5.97
MgO (%)	2.65	0.33	10.5	8.14	0.25	0.00
MnO (%)	0.14	0.02	0.41	0.53	0.05	0.08
CaO (%)	5.84	4.06	2.22	11.8	0.80	26.4
Na ₂ O (%)	3.08	4.24	0.66	1.18	0.12	0.26
K ₂ O (%)	2.36	2.12	6.92	1.39	0.14	0.05
P ₂ O ₅ (%)	0.62	0.35	0.23	0.11	0.08	2.31
S (%)	0.21	0.04	0.10	0.04	1.07	3.95
LOI (%)	0.45	0.50	1.60	0.39	0.00	3.23
TOTAL	98.75	98.07	95.99	96.93	102.00	101.94
Cr (ppm)	71	5	100	130	827	40
V (ppm)	187	25	336	382	1470	661
Ni (ppm)	28	4	99	44	72	38
Co (ppm)	20	3	28	32	55	>6000
Cu (ppm)	25.4	15.7	30.8	22.6	59.7	16.3
Zn (ppm)	98.6	17.0	366	240	75.4	13.4
Rb (ppm)	54.2	31.9	202	7.2	2.5	2.0
Sr (ppm)	855	1132	197	336	56.9	112
Zr (ppm)	159	121	43	45	9	22730
Nb (ppm)	15	9	4	6	5	237
Ba (ppm)	1770	2350	2430	156	89	37
Pb (ppm)	14.2	14.8	8.53	11.9	78.8	19.4
Th (ppm)	20.0	1.8	19.0	61.8	3.5	21.0
U (ppm)	<0.05	<0.05	<0.05	<0.05	<0.05	33.0
La (ppm)	152	36.3	202	715	66.0	386
Ce (ppm)	305	77.2	352	1300	133	1890
Nd (ppm)	143	27.0	68.4	258	45.9	1852
Sm (ppm)	20.2	4.30	5.57	24.5	4.59	401
Cl (ppm)	708	169	2060	2910	60	127

coarse, granular fabric of the rock. Biotite is dark brown, pleochroic, Fe-rich, high density, well formed, with good indication of hexagonal

outline. Hornblende is greenish, pleochroic with high Mg and high rare earth element (REE) content. Magnetite is Fe-rich with only a small quantity of associated ilmenite. Titanite occurs as translucent yellowish crystals some of which possess brown and black metamict regions, evidently lattice disruptions caused by significant radioactive decay of U or Th. Titanite, like hornblende, is strongly enriched in REEs. Other incompatible elements, like the REEs, appear to be enriched within hornblende and titanite. The most obvious exception is Rb that is enriched in the biotite, not hornblende and titanite.

The whole-rock elemental composition of this single sample of the Beartooth amphibolite resembles overall the “incompatible-element-rich andesitic amphibolite” generalized from the Beartooth Mountains of Wyoming and Montana [Mueller *et al.*, 1983]. The rare earth element (REE) pattern closely follows the generalized Beartooth amphibolites of Mueller *et al.* [1983], even in the enrichment of light REE over heavy REE. Titanium and Zr, elements that Mueller *et al.* [1983] argue are conserved during metamorphism, appear in the normal Beartooth abundance within our new rock sample. Because our new sample has significantly higher incompatible element concentration than the surrounding Long Lake granodiorite, the source of the incompatible elements cannot be the granodiorite at the time of the metamorphic event [Mueller *et al.*, 1983]. Strontium is also more abundant in the amphibolite than the surrounding granodiorite. Therefore, a case can be made that metamorphism was isochemical. Amphibolite retains its incompatible elements, including REEs and Sr, which were distinguishing characteristics of the rock before the metamorphic event. Hydrothermal alteration of the original andesite is not a viable explanation.

5.2 Bass Rapids Diabase Sill

The sill at Bass Rapids just east of Shinumo Creek is similar to other sills within the Unkar Group being composed of olivine diabase, but it is capped by granophyre (Figure 5), making this sill a classic example of in-place differentiation of a basaltic magma. The 6 m thick granophyre

consists predominantly of K-feldspar (55–60%) and quartz (12–25%), with biotite, plagioclase, some clinopyroxene, and titanomagnetite making up the remaining 20–28% [Snelling *et al.*, 2003]. The rock is holocrystalline, coarse-grained, and has a well-developed granophyric texture in which quartz, plagioclase, biotite, clinopyroxene and titanomagnetite fill interstices between the orthoclase crystals. The transition between the granophyre and diabase below occurs over a vertical distance of less than 1 m and is a zone rich in biotite and accessory minerals [Hendricks, 1989]. Apatite makes up as much as 5–10% of the rock. Ilmenite and titanite occur, and zircon with reaction halos is present within the biotite grains.

The olivine diabase interior of the sill is medium- to coarse-grained, containing plagioclase (30–45%), olivine (20–35%), clinopyroxene (15–30%), titanomagnetite and ilmenite (5%), and biotite (1%), with accessory apatite [Snelling *et al.*, 2003]. The texture is diabasic to subophitic, although a crude alignment of feldspar laths can be seen in many places. The plagioclase laths (composition An_{45-60} [45–60% anorthite]) average 1.5 mm in length and are partially to completely altered to sericite. Both normal and reverse zoning of crystals are common. Anhedral to subhedral olivine crystals up to 1 mm in diameter are often partially altered along borders and fractures to chlorite, talc, magnetite, iddingsite, and serpentine. Fresh grain interiors have compositions of approximately Fo_{80} (80% forsterite) and interference colors that suggest normal zoning. Plagioclase laths and olivine grains are often enclosed by large, optically continuous, poikilitic clinopyroxene grains, giving the rock its subophitic texture. The clinopyroxene is brownish-pink, non-pleochroic augite that is usually fresh. Large irregular grains of titanomagnetite partly altered to hematite and biotite, as well as primary pleochroic brown biotite partially altered to chlorite, occupy interstices between the plagioclase and olivine grains.

The olivine concentration tends to increase towards the center of the sill, whereas the clinopyroxene decreases. Immediately below the granophyre the diabase contains about 5% modal olivine, which increases rapidly to 20–30% through the central part of the sill [Hendricks and Lucchitta, 1974]. About 15 m above the base of the sill

is an olivine-rich layer that contains about 50% modal olivine, and then the olivine content of the diabase decreases to about 10% near the base. *Hendricks* [1989] and *Hendricks and Lucchitta* [1974] suggested that this distribution of the olivine in the sill can be explained by the process of flow differentiation, that involves the movement of early-formed olivine grains away from the margins of the sill during flow of the intruding magma [*Bhattacharji and Smith*, 1964; *Bhattacharji*, 1967; *Simkin*, 1967]. It is envisaged that, as the magma intrudes up through the conduit and then outward to form the sill, fluid-dynamic forces concentrate toward the center of the moving mass the already-formed olivine crystals, with crystal concentration occurring even before the emplacement of the sill. As the magma also moves laterally, gravity acting on the olivine crystals could have produced a gradational change in the olivine content from the lower contact upward, while causing an abrupt change in olivine from the upper contact downward. Once emplaced, crystallization of the remaining liquid magma within the sill would then have yielded the remaining minerals in relatively constant proportions [*Simkin*, 1967].

Although there is a general uniformity of the diabase throughout the sill, there are two types of textural variations described by *Noble* [1914]. First, there are “lumps” or “balls” similar in mineralogy to the surrounding diabase, that is, olivine and plagioclase with augite filling interstices. The plagioclase laths in the lumps are up to 7.5 mm in length, filling embayments in large olivine crystals. The augite occurs as ophitic intergrowths with the plagioclase. Second, pegmatite veins consisting of plagioclase and augite with a very similar texture are found in the upper part of the sill. These textural variations undoubtedly represent segregation features produced during crystallization of the sill.

The lower chilled margin and contact of the sill with the underlying Hakatai Shale is covered, but is probably similar to the fine-grained chilled margins found in most of the other sills intruding the Unkar Group in Grand Canyon. The upper contact of the sill is marked by the 6 m thick capping of granophyre, the contact with the overlying Hakatai Shale is sharp (Figure 5), and no xenoliths of Hakatai Shale are found in the granophyre, suggesting that it was not produced by assimilation of

the shale. Instead, the transition zone between the granophyre and the diabase beneath it in the sill suggests that the granophyre was a residual magma that “floated” to the top of the sill as the diabase crystallized, so that there was little late-stage mixing of it with the diabase part of the sill [Hendricks and Lucchitta, 1974].

Contact metamorphism of the Hakatai Shale has occurred above and below the sill, the shale being altered to a knotted hornfels (Figure 5). This contact metamorphism is greater below the sill than above it. The hornfels below the sill extends for 5 m below the contact and forms a prominent outcrop. Biotite porphyroblasts as much as 0.25 mm in size occur within 5 cm of the contact with the sill, and at 10 cm the shale is a knotted hornfels containing porphyroblasts of probable andalusite and cordierite that have been replaced pseudomorphically by muscovite and green chlorite respectively. These porphyroblasts become larger and less numerous away from the sill, reflecting a slower rate and lower density of nucleation. No recrystallization of the shale has occurred beyond 5 m below the sill contact, while the mineralogy of the metamorphism suggests that it was of low–medium grade.

The whole-rock, major element oxide and selected trace element data (Table 2) come from the full thickness of the sill (Figure 5). The major element oxide percentages are very similar to those reported by Hendricks [1989]. The granophyre as expected has a much higher SiO_2 content than the diabase making up the main portion of the sill, because the granophyre contains free quartz. Similarly, the diabase has a higher Fe_2O_3 and MgO content than the granophyre because of its olivine and augite content, the MgO concentration increasing towards the central part of the sill due to the higher olivine content there. Similarly, the higher Al_2O_3 and CaO values in the center of the sill would result from the concentration there of more calcic plagioclase. The high P_2O_5 content of sample DI-17 at the top of the diabase in close proximity to the granophyre is consistent with the apatite that is abundant in the transition zone. On a total alkalis-silica (TAS) diagram the diabase plots in the alkali olivine basalt field [Hendricks, 1989]. Larson *et al.* [1994], using their own data and that of Hendricks and Lucchitta [1974], suggested that chemically the diabase sills in the Unkar Group

Table 2. Whole-rock, major-element oxide and selected trace element analyses of eleven samples from the Bass Rapids sill, Grand Canyon, northern Arizona. Sample locations are shown in Figure 5. (Analyst: XRAL Laboratories of S.G.S. Canada, Don Mills, Ontario; January 1997 and February 2002.)

Oxide/ Element	Granophyre			Diabase							
	DI-10	DI-11	DI-16	DI-17	DI-15	DI-18	DI-14	DI-13	DI-19	DI-7	DI-22
	2 m below top	3.8 m below top	5.5 m below top	7.5 m below top	21 m below top	29 m below top	49 m below top	59 m below top	71 m below top	73 m below top	86 m below top
SiO ₂ (%)	60.4	60.9	57.8	46.5	45.4	46.0	45.2	44.7	44.5	45.2	46.2
TiO ₂ (%)	0.903	1.18	0.03	0.16	0.25	0.16	0.17	0.18	0.17	0.16	0.21
Al ₂ O ₃ (%)	14.8	15.4	14.2	11.6	13.8	15.8	14.0	14.6	12.8	15.7	14.9
Fe ₂ O ₃ (%)	5.96	4.79	8.24	16.2	14.1	12.5	13.3	12.4	12.6	10.3	13.5
MgO (%)	5.87	5.57	6.25	8.40	10.9	11.4	13.5	15.3	16.5	13.2	9.06
MnO (%)	<0.01	0.01	0.03	0.16	0.25	0.16	0.17	0.18	0.17	0.16	0.21
CaO (%)	0.27	0.09	0.65	4.16	6.89	8.13	7.68	7.80	4.16	8.48	7.15
Na ₂ O (%)	0.57	1.47	1.63	3.15	2.06	2.18	1.86	1.87	1.71	1.93	2.23
K ₂ O (%)	8.05	7.75	6.64	1.32	1.82	0.97	0.81	0.68	0.64	0.62	1.90
P ₂ O ₅ (%)	0.03	0.02	0.32	1.23	0.51	0.26	0.28	0.09	0.27	0.19	0.43
S (%)	0.007	0.004	0.02	0.03	0.12	0.15	0.12	0.03	0.09	0.052	0.10
LOI (%)	2.85	2.90	2.95	3.15	2.2	1.75	1.85	1.2	2.7	2.4	2.45
TOTAL	99.8	100.2	100.0	99.0	99.9	100.4	100.3	100.1	100.4	99.4	100.30
Cr (ppm)	55	14	69	52	237	326	317	395	460	400	165
V (ppm)	108	116	72	200	195	142	140	88	131	110	231
Ni (ppm)	31	11	30	25	214	244	317	455	558	478	191
Co (ppm)	15	12	21	38	62	68	64	67	83	69	56
Cu (ppm)	3.4	7.9	15.6	51.4	98.3	129	63.9	30.3	55.0	31.0	101
Zn (ppm)	23.1	33.8	48.4	79.0	203	88.3	78.6	81.3	116	82.5	125
Rb (ppm)	104	106	87	23	39	23	18	16	23	14	51
Sr (ppm)	36	34	113	168	342	470	363	441	379	441	395
Zr (ppm)	228	313	349	342	160	92	116	82	116	68	161
Nb (ppm)	16	18	10	11	8	4	6	3	5	21	7
Ba (ppm)	567	633	613	327	322	184	134	167	161	239	352
Pb (ppm)	<2	<2	<2	7	7	<2	<2	<2	3	<2	5
Th (ppm)	9.4	12.0	12.2	6.4	<0.5	2.3	2.3	0.7	2.4	0.6	1.2
U (ppm)	1.9	2.5	4.0	4.8	1.7	<0.5	1.3	0.9	1.9	<0.5	0.9
La (ppm)	36.6	31.9	29.4	39.5	15.5	7.1	8.2	3.6	7.5	7.3	11.9
Ce (ppm)	80.8	68.9	65.5	94.0	38.2	17.8	20.5	8.2	18.8	16.9	29.7
Nd (ppm)	38.0	31.6	34.4	59.4	24.2	11.7	13.1	6.0	11.9	10.6	19.4
Sm (ppm)	8.1	6.2	7.9	13.3	6.3	3.1	3.3	1.5	2.9	3.2	4.6
Cl (ppm)	430	600	1050	580	1620	835	1070	363	842	954	2690

exhibit similarities and dissimilarities with the lower-member flows of the Cardenas Basalt, which are commonly regarded as the extrusive

equivalents of these intrusive diabase sills.

Based on selected trace element data for one sample of the Hance Rapids sill, *Larson et al.* [1994] concluded that the variation in those data was very similar to trace element patterns for the lower-member flows of the Cardenas Basalt. The selected trace element data in Table 2 for the Bass Rapid diabase sill are also similar. Furthermore, the differences in trace element contents of the granophyre compared to the diabase are very obvious, and reflect the mineralogical differences. For example, Cr, Ni, Co, Cu, and Zn are much higher in the diabase than the granophyre, because of the olivine and trace sulfides found in the diabase that are not in the granophyre. In contrast, Ba, Rb, La, Ce, and Nd are much higher in the granophyre than in the diabase, reflecting differences in the feldspar contents of the two rock types, orthoclase being dominant in the granophyre, whereas plagioclase is dominant in the diabase and contains higher Sr. The higher content of Cl in the diabase parallels the higher content of P_2O_5 due to the presence of trace apatite. Zirconium is, as expected, higher in the granophyre where zircon is more likely to be in trace amounts.

6. Radioisotope Results for the Beartooth Amphibolite

The K-Ar analytical data and K-Ar model “ages” for Beartooth amphibolite are shown in Table 3. Potassium-Ar data were obtained for the whole rock and three mineral separates (quartz-plagioclase, biotite and hornblende). Although sufficient quantities of magnetite and titanite were obtained for the procedure, technical problems in acid digestion prevented K-Ar analysis of these two minerals. Potassium-Ar model ages within the three mineral phases from the single rock differ from 1520 ± 31 Ma (quartz-plagioclase) to 2620 ± 53 Ma (hornblende), with the whole rock giving a “model age” averaged from the minerals of 2011 ± 45 Ma (K-Ar model ages with assigned 1σ uncertainties). The model age method assumes no radiogenic ^{40}Ar was retained when the andesite cooled during the metamorphic event to form the amphibolite. Because it is extremely unlikely that the minerals of the amphibolite within a few centimeters of each other record a billion year cooling

Table 3. K-Ar data for the whole rock and selected minerals from the Beartooth andesitic amphibolite, sample BT-1, northwestern Wyoming. (Analyst: Dr. R. Reesman, Geochron Laboratories, Cambridge, Massachusetts.)

Sample	Sample Type	K ₂ O (wt%)	⁴⁰ K (ppm)	⁴⁰ K (mol/g) x 10 ⁻⁸	⁴⁰ Ar* (ppm)	⁴⁰ Ar* (mol/g) x 10 ⁻⁹	⁴⁰ Ar* (%)	total ⁴⁰ Ar (mol/g) x 10 ⁻⁹	³⁶ Ar (mol/g) x 10 ⁻¹³	Model Age (Ma)	Uncertainty (1σ error in Ma)
BT-1WR	whole rock	2.437	2.412	6.036	0.5180	12.96	96.6	13.42	15.57	2011	±45
BT-1QA	plagioclase/ quartz	1.951	1.931	4.832	0.2677	6.699	95.0	7.052	11.95	1520	±31
BT-1B	biotite	6.285	6.223	15.57	1.819	45.52	98.4	46.26	25.04	2403	±53
BT-1H	hornblende	1.305	1.292	3.233	0.4434	11.10	96.7	11.48	12.86	2620	±53

history, differential Ar loss can be supposed. The quartz-plagioclase fraction, that has lost the largest proportion of its ⁴⁰Ar, also has the lowest concentration of ³⁶Ar, consistent with an Ar loss model. Biotite and hornblende give the oldest “ages.” Biotite has significant ⁴⁰K and significant ⁴⁰Ar, differing from the other minerals. Although the biotite data could allow a K-Ar isochron plot, we assign little statistical significance to it and do not show it as a figure by *Isoplot*.

Rubidium-Sr, Sm-Nd, and Pb-Pb data for the Beartooth amphibolite are shown in Table 4. Figures 6, 7, and 8 are the three discordant mineral isochrons constructed by *Isoplot*. The Rb-Sr mineral isochron age (Figure 6) is 2515±110 Ma (2σ with expanded MSWD estimated errors) with initial ⁸⁷Sr/⁸⁶Sr for the rock of 0.7044. This initial

Table 4. Whole-rock and mineral Rb-Sr, Sm-Nd, and Pb-Pb radioisotopic data for the Beartooth andesitic amphibolite, sample BT-1, northwestern Wyoming. (Analyst: Assoc. Prof. G.L. Farmer, University of Colorado at Boulder.)

Sample	Sample Type	Rb (ppm)	Sr (ppm)	⁸⁷ Rb/ ⁸⁶ Sr	⁸⁷ Sr/ ⁸⁶ Sr	Sm (ppm)	Nd (ppm)	¹⁴⁷ Sm/ ¹⁴⁴ Nd	¹⁴³ Nd/ ¹⁴⁴ Nd	²⁰⁶ Pb/ ²⁰⁴ Pb	²⁰⁷ Pb/ ²⁰⁴ Pb	²⁰⁸ Pb/ ²⁰⁴ Pb
BT-1WR	Whole rock	54.2	855	0.183	0.70988	20.2	143	0.0856	0.510492	16.305	15.333	46.064
BT-1QA	Quartz and albite	31.9	1132	0.0816	0.70602	4.3	27.0	0.0963	0.510790	14.455	15.007	35.618
BT-1B	Biotite	202	197	3.00	0.81352	5.57	68.4	0.0492	0.509852	16.342	15.333	63.045
BT-1H	Hornblende	7.2	336	0.0620	0.70892	24.5	258	0.0574	0.509981	16.610	15.412	90.22
BT-1M	Magnetite	2.5	56.9	0.127	0.71025	4.59	45.9	0.0605	0.510703	17.108	15.485	37.546
BT-1T	Titanite	2.0	112	0.0517	0.70525	401	1852	0.131	0.511381	165.587	42.666	97.878
BT-1T2	Titanite	1.0	75	0.0380	0.70427	487	2152	0.1369	0.511412	173.759	44.466	93.366

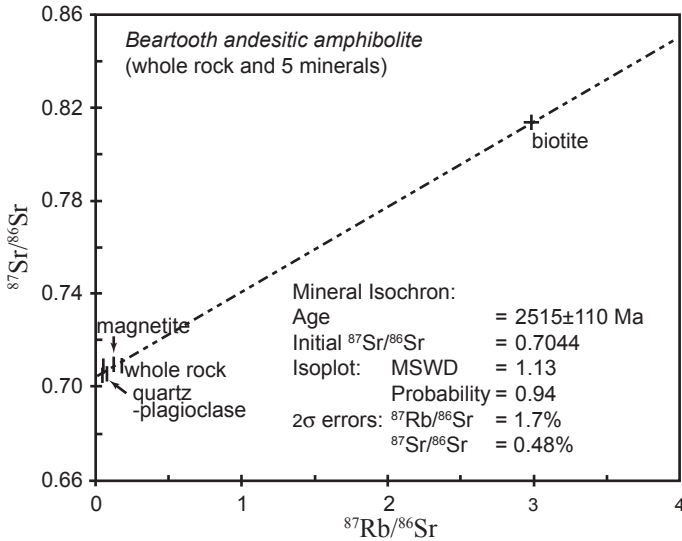


Figure 6. Rb-Sr mineral isochron for the Beartooth andesitic amphibolite. Error bars in this and following plots are 2σ .

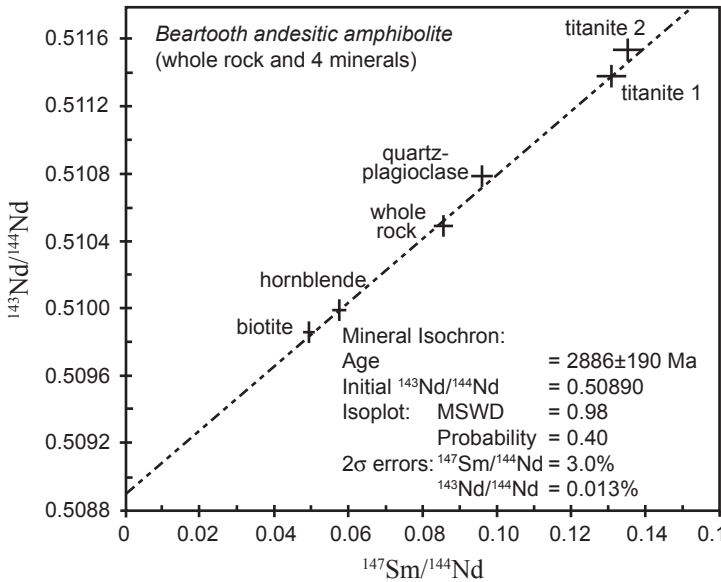


Figure 7. Sm-Nd mineral isochron for the Beartooth andesitic amphibolite. The mineral separate called “titanite 2” was not used in the regression analysis.

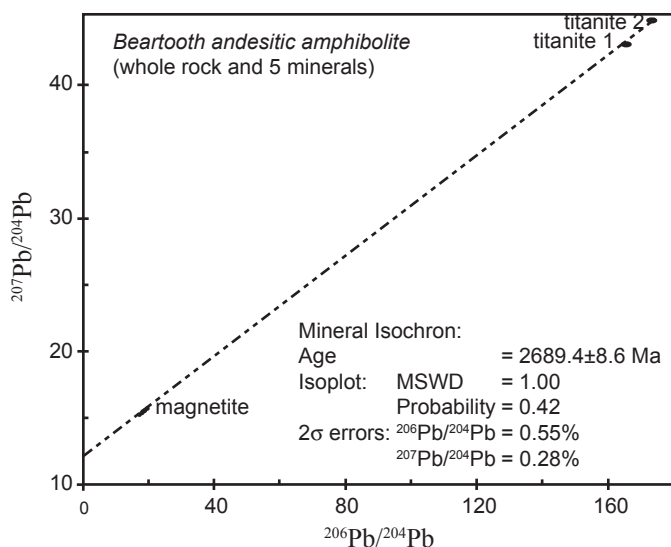


Figure 8. Pb-Pb mineral isochron for the Beartooth andesitic amphibolite. Both “titanite 1” and “titanite 2” were included in the regression analysis. Error ellipses (2σ) are very small at the scale of the plot.

$^{87}\text{Sr}/^{86}\text{Sr}$ is slightly higher than the value of 0.7022 obtained regionally by the whole-rock isochron of *Wooden et al.* [1982]. The Rb-Sr mineral isochron age is discordant with the 28-point Rb-Sr whole-rock isochron of *Wooden et al.* [1982]. This 6-point mineral isochron in Figure 6, although largely determined by the biotite and including magnetite, has an MSWD near unity and high probability. Figure 7 is the 5-point Sm-Nd mineral isochron of 2886 ± 190 Ma, discordant from Rb-Sr. The mineral magnetite (without significant ilmenite included) appears to lie off the line described by the other five points, suggesting that the magnetite did not remelt completely in the metamorphic process, but retained its initial $^{143}\text{Nd}/^{144}\text{Nd}$ from the protolith, not from the homogenization of the subsequent metamorphic event. The 5-point Sm-Nd mineral isochron in Figure 7 has an MSWD near unity (indicating assigned errors are properly stated) and acceptable probability. The spread of the data in Figure 7 is very good, with titanite being strongly enriched in light REEs thus producing a higher $^{147}\text{Sm}/^{144}\text{Nd}$ beneficial to the isochron. Because of the technical difficulty of measuring very high abundances

of Sm and Nd in titanite, two separate splits of titanite were submitted for Sm-Nd analysis. Although the second sample was reprocessed to produce a higher purity sample (BT-1T2), general agreement between these measurements indicates accuracy. Only one titanite sample (BT-1T) was used for the regression analysis. Figure 8 is the Pb-Pb mineral isochron of 2689 ± 9 Ma, including magnetite and two separate splits and measurements of the extremely radiogenic Pb of titanite. The MSWD is unity (indicating assigned errors are properly stated) and *Isoplot* calculates acceptable probability. The Pb-Pb mineral isochron has very low error associated with the estimated age because of the extreme difference in radiogenic Pb's between the minerals, and because the isochron interpretation supposes the radiogenic Pb's to have been homogenized during the essentially instantaneous metamorphic event. The Pb-Pb mineral isochron for Beartooth amphibolite is discordant with the Rb-Sr mineral isochron and the whole-rock Rb-Sr isochron of *Wooden et al.* [1982]. Also, the Sm-Nd mineral isochron is discordant with the Rb-Sr mineral isochron.

7. Radioisotope Results for the Bass Rapids Diabase Sill

7.1 K-Ar Data

The K-Ar analytical data and K-Ar model "ages" for all eleven samples are listed in Table 5. These model ages are calculated by the standard equation of *Dalrymple and Lanphere* [1969] using the ratio of the abundances of $^{40}\text{Ar}^*$ (the radiogenic ^{40}Ar) to ^{40}K listed in Table 5. The model age method assumes no radiogenic ^{40}Ar was present when the basaltic magma cooled to form the diabase sill. The model "ages" range from 656 ± 15 Ma to 1053 ± 24 Ma (1σ age errors derived from analytical errors only), with the mean age being 816 Ma ($n = 11$). Model ages with such wide variation are difficult to explain, because they are not easily predicted by any possible sequence in the formation of the sill, such as the bottom and top of the sill cooling before the center of the sill, or the granophyre cooling before the diabase below. Indeed, there is no recognizable pattern, except that the model "ages" are discordant

Table 5. K-Ar data for whole rocks from the Bass Rapids diabase sill, Grand Canyon, northern Arizona. (Analysts: Dr. R. Reesman, Geochron Laboratories, Cambridge, Massachusetts, and Dr. Y. Kapusta, Activation Laboratories, Ancaster, Canada.)

Sample	Rock Type	Position (from top)	K ₂ O (wt%)	⁴⁰ K (ppm)	⁴⁰ K (mol/g) × 10 ⁻⁸	⁴⁰ Ar* (ppm)	⁴⁰ Ar* (mol/g) × 10 ⁻⁹	⁴⁰ Ar* (%)	total ⁴⁰ Ar (mol/g) × 10 ⁻⁹	³⁶ Ar (mol/g) × 10 ⁻¹³	Model Age (Ma)	Uncertainty (1σ error in Ma)
DI-10	Granophyre	2m	8.61	8.527	21.34	0.5737	14.36	96.4	14.90	18.27	895	±20
DI-11		3.8m	8.245	8.166	20.43	0.4206	10.52	94.3	11.16	21.66	721	±14
DI-16		5.5m	5.764	5.706	14.28	0.4281	10.71	92.85	11.53	27.75	974	±20
DI-17	Diabase	7.5m	1.413	1.399	3.501	0.1162	2.908	86.4	3.366	15.50	1053	±24
DI-15		21m	2.661	2.634	6.591	0.1211	3.030	86.15	3.517	16.48	656	±15
DI-18		29m	1.356	1.342	3.358	0.06572	1.645	76.45	2.152	17.16	692	±14
DI-14		49m	0.959	0.950	2.377	0.06567	1.643	76.1	2.159	17.46	914	±22
DI-13		59m	0.958	0.948	2.372	0.05014	1.255	83.45	1.504	8.426	737	±18
DI-19		71m	0.778	0.770	1.926	0.04973	1.244	75.8	1.641	13.44	866	±24
DI-7		73m	0.754	0.747	1.869	0.03893	0.9742	80.0	1.218	8.250	728	±20
DI-22		86m	2.157	2.135	5.343	0.11107	2.779	91.21	3.047	9.069	740	±22

from one another. The mean model “age” for the granophyre is 863 Ma ($n = 3$), whereas the mean model “age” for the diabase is 798 Ma ($n = 8$), but the model “age” for sample DI-14 in the center of the diabase sill is much older at 914 ± 22 Ma. Furthermore, pairs of samples very close to one another give highly discordant model “ages,” such as granophyre samples DI-10 and DI-11 which are only 1.8 m apart and yet yield model “ages” of 895 ± 20 Ma and 721 ± 14 Ma respectively, and diabase samples DI-19 and DI-7 which are only 2 m apart and, yet, yield model “ages” of 866 ± 24 Ma and 728 ± 20 Ma respectively.

Figure 9 is the ⁴⁰K versus ⁴⁰Ar* diagram for the Bass Rapids diabase sill. The error bars plotted with the data are the estimated 2σ uncertainties, and the strong linear trend that is apparent is plotted as an isochron using the *Isoplot* program of Ludwig [2001] that utilizes the least-squares linear regression method of York [1969]. All eleven samples were included in the regression calculation, although the assigned 2σ errors were large. The isochron “age” calculated from the slope of the line is 841.5 ± 164 Ma (2σ error). The initial ⁴⁰Ar is zero, so this is consistent with the assumption of zero ⁴⁰Ar* in the model age technique. This K-Ar isochron “age” is discordant with the published

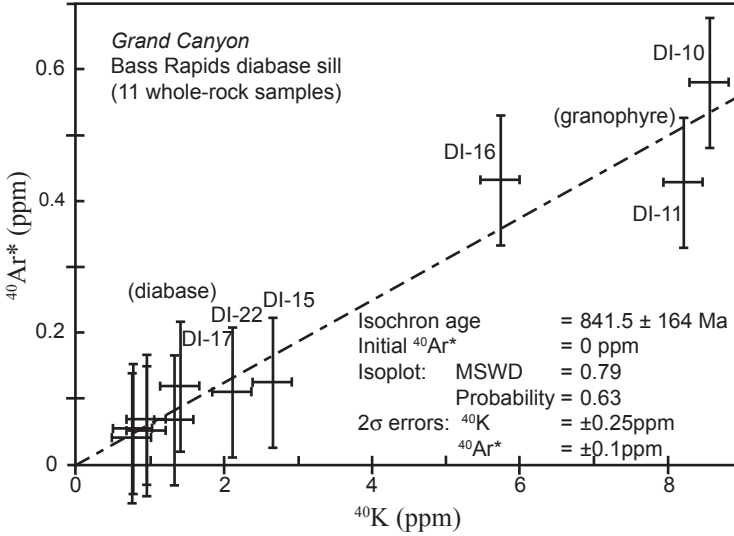


Figure 9. ^{40}K versus $^{40}\text{Ar}^*$ in the Bass Rapids diabase sill, all eleven samples being used in the isochron and age calculation. The bars represent 2σ uncertainties.

five-point Rb-Sr whole-rock isochron “age” for the sill of 1070 ± 30 Ma [Elston and McKee, 1982]. Note also that the slope of the line is heavily influenced by the three granophyre data points with their high K contents due to their contained orthoclase. Because all the samples are cogenetic it was important that all be included in the calculation, even though it leads to a large 2σ uncertainty in the isochron age. This large uncertainty must be due to more than analytical errors, and is thus indicative of the minor hydrothermal alteration present (plagioclase altered to sericite) and perhaps some contamination of the granophyre from the hornfels wall-rock during contact metamorphism.

Figure 10 shows $^{40}\text{K}/^{36}\text{Ar}$ plotted against $^{40}\text{Ar}/^{36}\text{Ar}$ for the sill, based on the data in Table 5. The error bars again represent the 2σ uncertainties in the data points, which again are large, with all eleven samples included in the regression analysis. The calculated isochron “age” is therefore 840.4 ± 179 Ma with an initial $^{40}\text{Ar}/^{36}\text{Ar}$ value of 214. This is much less than the present atmospheric $^{40}\text{Ar}/^{36}\text{Ar}$ value of 295.5, and suggests the possibility of a small Ar loss or that the regression

line needs to be appropriately adjusted. This would reduce the isochron age, and make it even more discordant with the published Rb-Sr whole-rock isochron age, even though it would still be concordant with the K-Ar isochron age determined here and shown in Figure 9. Alternately, the low $^{40}\text{Ar}/^{36}\text{Ar}$ value could indicate incorporation into the basaltic magma of “primitive argon” thus inherited from its mantle source [Dalrymple, 1969].

7.2 Rb-Sr Data

The whole-rock Rb-Sr, Sm-Nd and Pb-Pb radioisotope data for all eleven samples from the sill are listed in Table 6. As anticipated, the radioisotope ratios in the three granophyre samples are distinctly

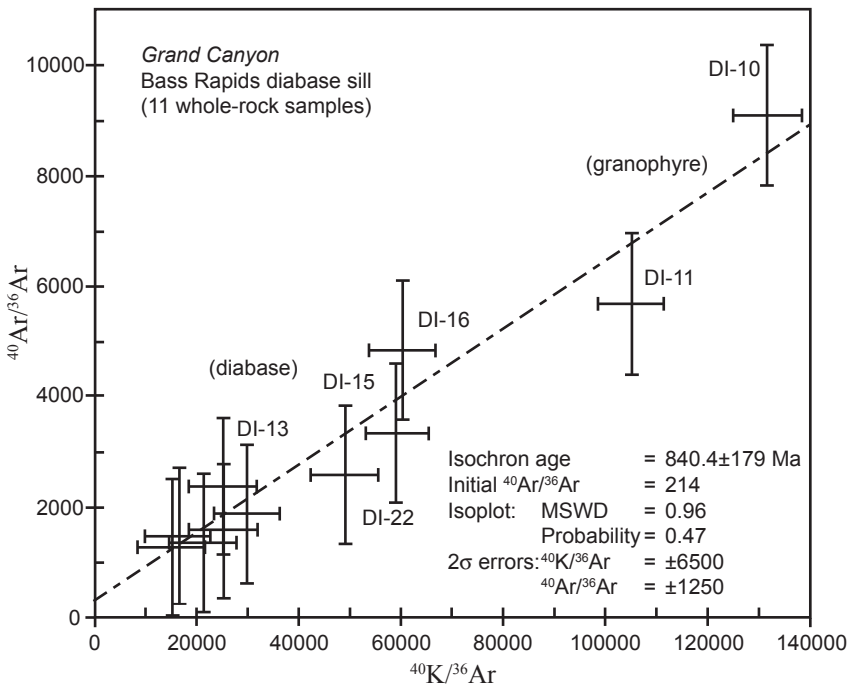


Figure 10. $^{40}\text{K}/^{36}\text{Ar}$ versus $^{40}\text{Ar}/^{36}\text{Ar}$ in the Bass Rapids diabase sill, all eleven samples being used in the isochron and age calculation. The bars represent 2σ uncertainties.

Table 6. Whole-rock Rb-Sr, Sm-Nd, and Pb-Pb radioisotopic data for the Bass Rapids diabase sill, Grand Canyon, northern Arizona. (Analyst: Assoc. Prof. G.L. Farmer, University of Colorado at Boulder.)

Sample	Rock Type	Position (from top)	Rb (ppm)	Sr (ppm)	$^{87}\text{Rb}/^{86}\text{Sr}$	$^{87}\text{Sr}/^{86}\text{Sr}$	Sm (ppm)	Nd (ppm)	$^{147}\text{Sm}/^{144}\text{Nd}$	$^{143}\text{Nd}/^{144}\text{Nd}$	$^{206}\text{Pb}/^{204}\text{Pb}$	$^{207}\text{Pb}/^{204}\text{Pb}$	$^{208}\text{Pb}/^{204}\text{Pb}$
DI-10	Granophyre	2m	101.5	35	8.4302	0.83703	8.25	37.8	0.132	0.512070	22.948	15.933	42.233
DI-11		3.8m	95.8	33	8.439	0.82481	8.11	32.59	0.150	0.511992	25.432	16.135	45.201
DI-16		5.5m	82.8	106	2.2643	0.741297	7.98	36.3	0.1329	0.512084	21.923	15.878	41.482
DI-17	Diabase	7.5m	24.2	154	0.4539	0.713329	14.55	62.4	0.1411	0.512391	19.368	15.702	38.574
DI-15		21m	38.5	312	0.3568	0.709139	6.0	25.0	0.1456	0.512441	17.255	15.475	36.981
DI-18		29m	21.8	422	0.1492	0.706359	3.08	12.5	0.1495	0.512458	17.358	15.494	37.003
DI-14		49m	11.7	328	0.1026	0.705461	3.37	13.8	0.1473	0.512443	18.355	15.561	38.154
DI-13		59m	15.4	383	0.1165	0.704818	2.65	10.8	0.1480	0.512438	17.699	15.510	37.353
DI-19		71m	16.9	329	0.1487	0.705019	3.60	15.0	0.1452	0.512466	17.260	15.452	36.854
DI-7		73m	11.5	347	0.0959	0.704502	1.64	6.04	0.164	0.512554	17.407	15.480	37.005
DI-22		86m	51.3	371	0.4005	0.711306	5.13	21.1	0.1471	0.512446	19.429	15.687	38.711

different from those obtained in the eight diabase samples. This reflects the major and trace element differences between these two rock types and their different mineralogies, the granophyre having a much higher K_2O content than the diabase because of the abundant orthoclase in it (Table 5). Thus, the Rb content of the granophyre is higher than that of the diabase, whereas the Sr content is higher in the diabase because it partitions with the Ca in plagioclase (Table 6). The generally higher REE and Pb contents of the granophyre likewise cause significantly different radioisotope ratios in the granophyre compared to the diabase. These differences are ideal for plotting of isochrons because of the larger spreads in the radioisotope ratios.

Figure 11 shows $^{87}\text{Rb}/^{86}\text{Sr}$ plotted against $^{87}\text{Sr}/^{86}\text{Sr}$ for the whole-rocks of the sill, based on the data in Table 6. The error bars again represent the 2σ uncertainties in the data points, which were small. The regression analysis using the *Isoplot* program of Ludwig [2001] yielded an excellent-fitting isochron with a high probability and MSWD near unity. The resultant isochron “age” of 1055 ± 46 Ma is only marginally less than the five-point Rb-Sr isochron “age” of 1070 ± 30 Ma obtained by Elston and McKee [1982]. At 0.7043, the initial $^{87}\text{Sr}/^{86}\text{Sr}$ for this isochron is virtually identical to the value of 0.70420 ± 0.0007 obtained by Elston and McKee [1982]. Significantly, when we added the

Rb-Sr data for the five Elston and McKee samples to that of our eleven samples the resulting regression analysis yielded an even better sixteen-point isochron with a higher probability (0.86) from the same 2σ uncertainties for each of the data points. The isochron “age” of 1055 ± 44 Ma is identical, as is the initial $^{87}\text{Sr}/^{86}\text{Sr}$. Nevertheless, the uncertainty of ± 44 Ma is higher than the ± 30 Ma obtained by *Elston and McKee* [1982], but a lot of this uncertainty is due to the poorer fit of the two high Rb granophyre samples DI-10 and DI-11. Our uncertainties also assume more sources of error than those assigned by Elston and McKee, and our uncertainties appear to be better justified by our larger data set.

Rubidium-Sr data for minerals separated from the whole-rock diabase samples appear in Tables 7 and 8. Six mineral phases were separated from whole rock DI-13, and eleven mineral phases were separated from whole rock DI-15. In addition to magnetite separated from diabase whole rocks DI-13 and DI-15, magnetite was also separated from two other diabasites (DI-7 and DI-17) and all three granophyres (DI-10,

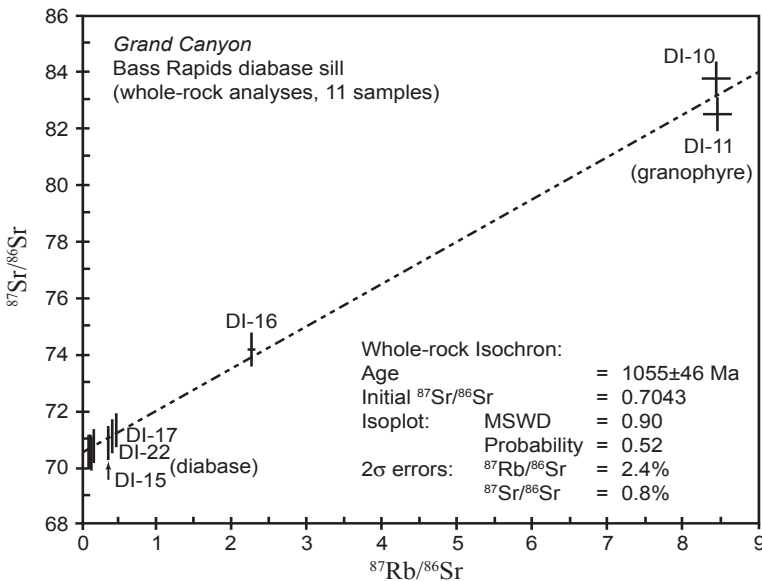


Figure 11. Rb-Sr whole-rock isochron for the Bass Rapids diabase sill. The bars represent 2σ uncertainties.

Table 7. Mineral Rb-Sr, Sm-Nd, and Pb-Pb radioisotopic data for diabase sample DI-13 from the Bass Rapids sill, Grand Canyon, northern Arizona. (Analyst: Assoc. Prof. G. L. Farmer, University of Colorado at Boulder.)

DI-13 fraction	Rb (ppm)	Sr (ppm)	⁸⁷ Rb/ ⁸⁶ Sr	⁸⁷ Sr/ ⁸⁶ Sr	Sm (ppm)	Nd (ppm)	¹⁴⁷ Sm/ ¹⁴⁴ Nd	¹⁴³ Nd/ ¹⁴⁴ Nd	²⁰⁶ Pb/ ²⁰⁴ Pb	²⁰⁷ Pb/ ²⁰⁴ Pb	²⁰⁸ Pb/ ²⁰⁴ Pb
Whole-rock	15.4	383	0.1165	0.704818	2.65	10.8	0.1480	0.512438	17.699	15.510	37.353
Biotite	92.2	187	1.4294	0.724746	2.37	11.3	0.1266	0.512225	17.457	15.486	37.150
Clinopyroxene	0.74	32.8	0.0651	0.704166	5.19	14.3	0.2190	0.512922	17.463	15.477	37.191
Plagioclase	28.5	784	0.1050	0.704769	0.63	9.4	0.0408	0.511448	17.194	15.471	36.913
High-density Plagioclase	27.3	634	0.1244	0.704967	8.96	39.1	0.1385	0.512403	17.085	15.461	36.791
Olivine	0.36	7.62	0.1348	0.704752	1.15	5.9	0.1189	0.512097	17.384	15.536	37.171
Magnetite (+ilmenite)	1.01	7.98	0.3669	0.708408	0.88	27.1	0.0196	0.511161	18.423	15.640	38.035

DI-11 and DI-16). All this magnetite data is shown in Table 9. The strong partitioning of the relevant trace elements into the different mineral phases is evident as expected. For example, Rb is high in the biotite, whereas the Sr is high in the plagioclase. This was expected to provide a good spread in the radioisotopic data, and improve the statistics of the

Table 8. Mineral Rb-Sr, Sm-Nd, and Pb-Pb radioisotopic data for diabase sample DI-15 from the Bass Rapids sill, Grand Canyon, northern Arizona. (Analyst: Assoc. Prof. G. L. Farmer, University of Colorado at Boulder.)

DI-15 fraction	Rb (ppm)	Sr (ppm)	⁸⁷ Rb/ ⁸⁶ Sr	⁸⁷ Sr/ ⁸⁶ Sr	Sm (ppm)	Nd (ppm)	¹⁴⁷ Sm/ ¹⁴⁴ Nd	¹⁴³ Nd/ ¹⁴⁴ Nd	²⁰⁶ Pb/ ²⁰⁴ Pb	²⁰⁷ Pb/ ²⁰⁴ Pb	²⁰⁸ Pb/ ²⁰⁴ Pb
Whole-rock	38.5	312	0.3568	0.709139	6.0	25.0	0.1456	0.512441	17.255	15.457	36.981
Biotite	114.01	90.7	3.651	0.760260	2.59	13.7	0.1145	0.512107	18.258	15.595	37.967
Hornblende	0.85	36.0	0.068	0.704743	6.47	18.4	0.2125	0.512924	17.478	15.531	37.185
Heavy Hornblende	3.02	53.7	0.1625	0.706273	6.62	24.8	0.1617	0.512512	17.524	15.497	37.241
Clinopyroxene	0.88	38.2	0.0663	0.704856	7.13	21.4	0.2017	0.512857	17.427	15.474	37.068
Heavy Clinopyroxene	3.2	55.7	0.1661	0.706477	6.61	22.2	0.1805	0.512664	17.457	15.500	37.267
Orthopyroxene	11.4	343.3	0.0937	0.705124	274	1188	0.1395	0.512397	17.624	15.545	37.419
Plagioclase	78.8	649	0.351	0.709055	1.41	6.7	0.1265	0.511850	17.445	15.579	37.145
High-density Plagioclase	61.1	549	0.3214	0.708425	73.4	345	0.1287	0.512401	17.742	15.506	37.445
Olivine	1.0	4.2	0.441	0.709888	1.59	6.4	0.1506	0.511808	17.398	15.600	37.311
Magnetite	2.4	124	0.0552	0.706713	0.44	2.3	0.1194	0.511910	17.613	15.515	37.425
Ilmenite	0.69	5.4	0.3712	0.709848	0.37	1.7	0.1299	No data	19.275	15.671	38.429

Table 9. Magnetite and ilmenite Rb-Sr, Sm-Nd, and Pb-Pb radioisotopic data for the Bass Rapids diabase sill, Grand Canyon, northern Arizona. (Analyst: Assoc. Prof. G. L. Farmer, University of Colorado at Boulder.)

Magnetite Sample (ilmenite status)	Host Rock	Rb (ppm)	Sr (ppm)	$^{87}\text{Rb}/^{86}\text{Sr}$	$^{87}\text{Sr}/^{86}\text{Sr}$	Sm (ppm)	Nd (ppm)	$^{147}\text{Sm}/^{144}\text{Nd}$	$^{143}\text{Nd}/^{144}\text{Nd}$	$^{206}\text{Pb}/^{204}\text{Pb}$	$^{207}\text{Pb}/^{204}\text{Pb}$	$^{208}\text{Pb}/^{204}\text{Pb}$
DI-10 MAG (+ILM)	Granophyre	8.2	4.0	6.443	0.797199	3.03	18.3	0.1004	0.511898	20.021	15.83	39.556
DI-11 MAG (+ILM)		3.03	4.6	1.9021	0.734262	5.32	39.6	0.0814	0.511733	22.152	16.181	41.246
DI-16 MAG (+ILM)		4.7	11	1.21	0.726166	4.32	23.5	0.1111	0.511970	22.959	15.988	40.543
DI-17 MAG (+ILM)	Diabase	1.3	9.0	0.3933	0.715454	2.03	9.3	0.1325	0.512179	20.033	15.765	39.325
DI-15 MAG (-ILM)		2.4	124	0.0552	0.706713	0.44	2.3	0.1194	0.511910	17.613	15.515	37.425
DI-15 ILM (-MAG)		0.69	5.4	0.3712	0.709848	0.37	1.7	0.1299	No data	19.275	15.671	38.429
DI-13 MAG (+ILM)		1.01	7.98	0.3669	0.708408	0.88	27.1	0.0196	0.511161	18.423	15.640	38.035
DI-7 HM (-ILM)		2.4	34	0.2893	0.70578	1.72	9.69	0.107	0.512160	18.158	15.585	37.738

isochron fits. For the specific Rb-Sr plots in Figures 12 through 14, we plotted all the Rb-Sr mineral data at the same scale as the Rb-Sr whole-rock data (Figure 11) so the extraordinary linearity of the data can be better appreciated.

Figure 12 is the $^{87}\text{Rb}/^{86}\text{Sr}$ versus $^{87}\text{Sr}/^{86}\text{Sr}$ diagram for the six mineral fractions from sample DI-13, plus the whole rock, plotted on the same scale as the whole rocks. The regression analysis produced an excellent isochron fit, with good probability and MSWD near unity. The resultant isochron “age” is 1060 ± 24 Ma, the 2σ uncertainty being low because the 2σ error bars on the data points are also low, and the data spread, thanks to the biotite, is high. This mineral isochron age is, of course, totally concordant with the whole-rock Rb-Sr isochron “age” (1055 ± 46 Ma, Figure 11), but at 0.70301 the initial $^{87}\text{Sr}/^{86}\text{Sr}$ is marginally lower than that for the whole-rock isochron.

Figure 13 is the $^{87}\text{Rb}/^{86}\text{Sr}$ versus $^{87}\text{Sr}/^{86}\text{Sr}$ diagram for the eleven mineral fractions from sample DI-15, plus the whole rock. Again, the regression analysis, when plotted on the same scale as the whole rocks, produces an excellent isochron fit, with good probability and MSWD near unity.

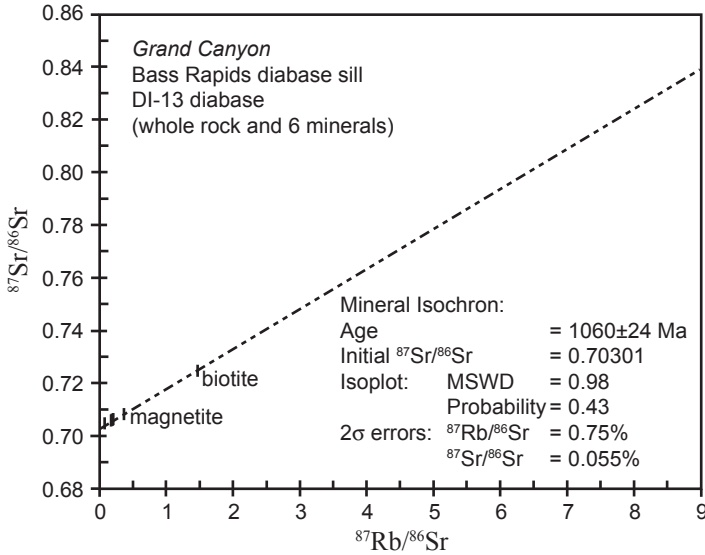


Figure 12. Rb-Sr mineral isochron for diabase sample DI-13 from the Bass Rapids diabase sill. The bars represent 2 σ uncertainties. This age has the most tightly constrained error obtained from the sill.

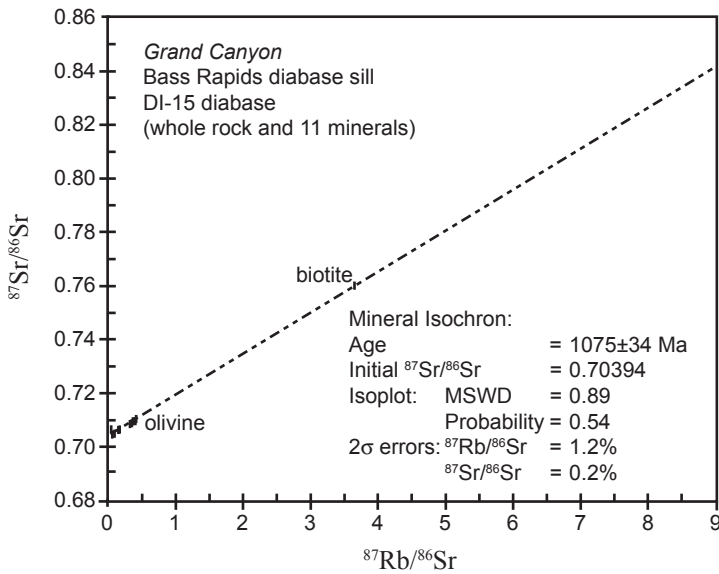


Figure 13. Rb-Sr mineral isochron for diabase sample DI-15 from the Bass Rapids diabase sill. The bars represent 2 σ uncertainties.

The resultant isochron “age” is 1075 ± 34 Ma, the 2σ uncertainty being low. This mineral isochron age is concordant with the whole-rock Rb-Sr isochron “age” (1055 ± 46 Ma, Figure 11), but at 0.70394 the initial $^{87}\text{Sr}/^{86}\text{Sr}$ is also marginally lower than that for the whole-rock isochron. This mineral isochron age is also concordant with the Rb-Sr mineral isochron age from DI-13 (1060 ± 24 Ma, Figure 12), with essentially the same initial Sr ratio.

Figure 14 is the Rb-Sr magnetite mineral isochron assembled from the various rocks. This plot includes all seven magnetites plus the ilmenite from DI-15. As expected, the magnetites from the granophyre (samples DI-10, DI-11, and DI-16) are more radiogenic than the magnetites and ilmenite from the diabase samples. *Isoplot* gives the magnetite mineral isochron “age” of 1007 ± 79 Ma, marginally less but still concordant with the most robust Rb-Sr mineral isochron from sample DI-13 (1060 ± 24 Ma, Figure 12).

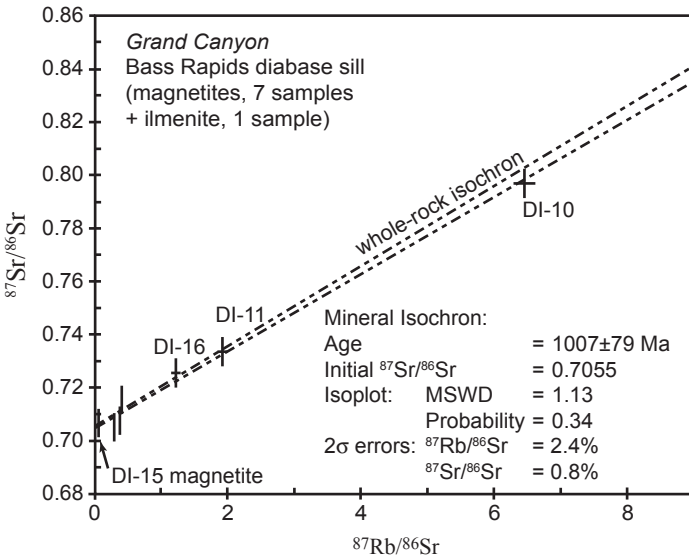


Figure 14. Rb-Sr magnetite mineral isochron for the Bass Rapids diabase sill. The bars represent 2σ uncertainties. The whole-rock Rb-Sr isochron is shown for comparison.

7.3 Sm-Nd Data

Figure 15 is the $^{147}\text{Sm}/^{144}\text{Nd}$ versus $^{143}\text{Nd}/^{144}\text{Nd}$ diagram for the Bass Rapids diabase sill using the whole-rock data in Table 6. These whole-rock samples are tightly grouped showing that little variation within the Sm-Nd system exists within the whole rocks. No Sm-Nd age information can be derived from the eleven whole-rock samples. All eight diabase samples do suggest a line in Figure 15, but *Isoplot* [Ludwig, 2001] attaches little age significance to it. The DI-13 Sm-Nd mineral isochron (see below) is plotted in Figure 15 and appears to pass through the eight whole-rock diabase samples. The three granophyre samples (DI-10, DI-11, and DI-16) plot on the diagram in a random

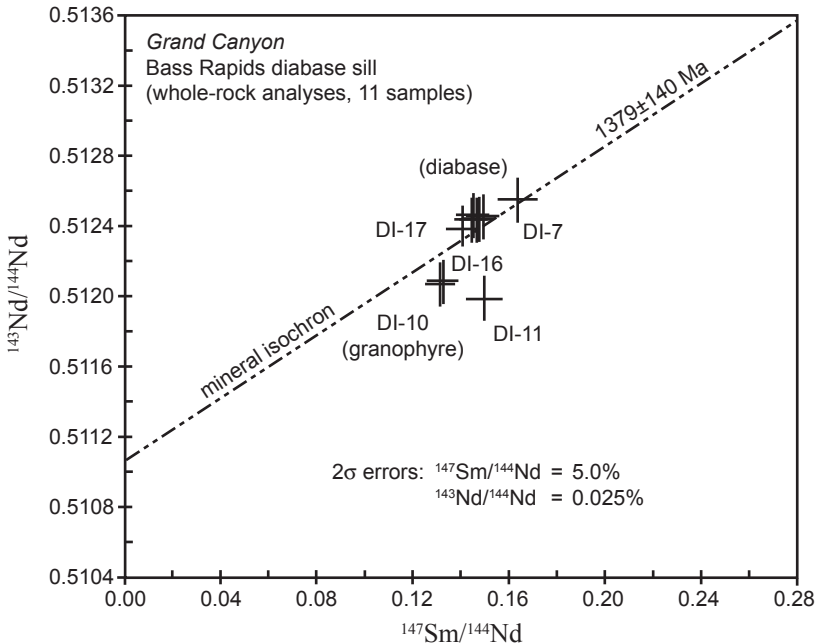


Figure 15. $^{147}\text{Sm}/^{144}\text{Nd}$ versus $^{143}\text{Nd}/^{144}\text{Nd}$ diagram for all eleven whole-rock samples of the Bass Rapids diabase sill. The bars represent the 2σ uncertainties. The Sm-Nd mineral isochron of Figure 16 is shown for comparison. The eight diabase samples plot on the mineral isochron whereas the three granophyre samples (DI-10, DI-11, and DI-16) do not, suggesting they have been contaminated from the hornfels wall rock.

scatter widely separated from any apparent relationship with the eight diabase samples, which is suggestive of contamination of the feldspar from the overlying hornfels wall rock, perhaps by some assimilation of less radiogenic Nd. Magnetite mineral data for the three granophyre samples (DI-10, DI-11, and DI-16) reported in Table 9 supports this interpretation. If we suppose that the magnetite of granophyre samples DI-10, DI-11, and DI-16 reflects the whole-rock Sm-Nd, we can plot those magnetites as a proxy for each of the altered whole-rocks. The Sm-Nd of the three magnetites of the granophyres do appear to plot on the line with the normal diabase whole-rocks.

Figure 16 shows the $^{147}\text{Sm}/^{144}\text{Nd}$ versus $^{143}\text{Nd}/^{144}\text{Nd}$ diagram for the six mineral fractions, plus the whole rock, of sample DI-13 from the Bass Rapids diabase sill. These Sm-Nd data are plotted at the same scale as the

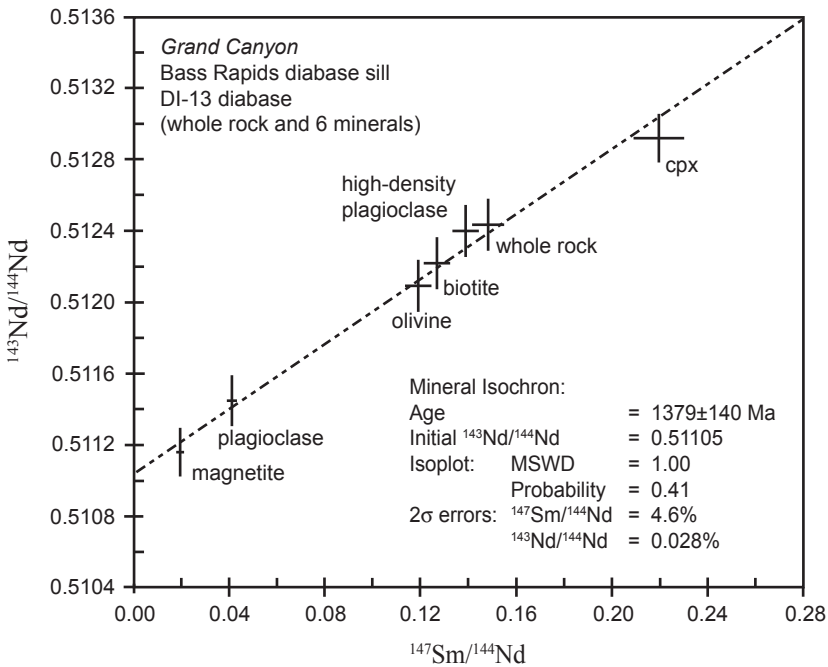


Figure 16. $^{147}\text{Sm}/^{144}\text{Nd}$ versus $^{143}\text{Nd}/^{144}\text{Nd}$ diagram for six mineral fractions from diabase sample DI-13 (plus the whole rock) from the Bass Rapids diabase sill. All seven data points were used in the isochron and age calculations, and the bars represent the 2σ uncertainties.

Sm-Nd of the whole rocks. The diagram shows an excellent large spread among the seven data points, from magnetite with the lowest $^{147}\text{Sm}/^{144}\text{Nd}$ ratio through to the highest $^{147}\text{Sm}/^{144}\text{Nd}$ ratio in the clinopyroxene. The regression analysis again produced an excellent isochron fit with a good probability and MSWD exactly unity. The resultant mineral isochron “age” for DI-13 is 1379 ± 140 Ma that is strongly discordant with the four robust Rb-Sr isochrons. The relatively large 2σ uncertainty in the isochron age is of course due to the relatively large 2σ error bars for each of the data points, and to the scatter of some of the data points (for example, the whole rock and clinopyroxene) either side of the isochron (the line of best fit).

Figure 17 shows the $^{147}\text{Sm}/^{144}\text{Nd}$ versus $^{143}\text{Nd}/^{144}\text{Nd}$ diagram for eight of the eleven mineral fractions, plus the whole rock, of sample DI-15.

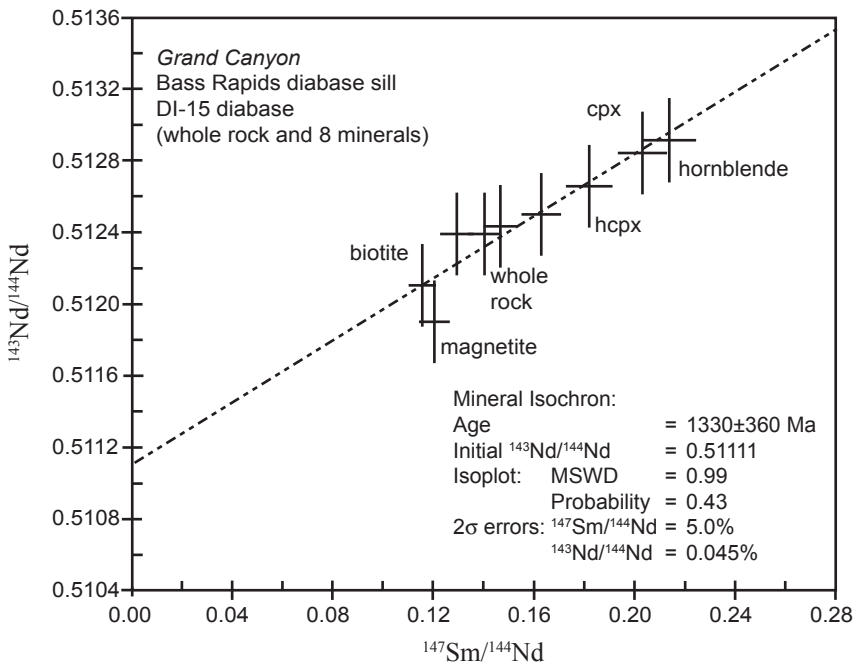


Figure 17. $^{147}\text{Sm}/^{144}\text{Nd}$ versus $^{143}\text{Nd}/^{144}\text{Nd}$ diagram for eight mineral fractions from diabase sample DI-15 (plus the whole rock) from the Bass Rapids diabase sill. Nine data points were used in the isochron and age calculations, and the bars represent the 2σ uncertainties.

These Sm-Nd data are plotted at the same scale as the Sm-Nd of the whole rocks and the minerals in DI-13. The diagram shows moderate spread among the nine data points, from biotite with the lowest $^{147}\text{Sm}/^{144}\text{Nd}$ ratio through to the highest $^{147}\text{Sm}/^{144}\text{Nd}$ ratio in the hornblende. The regression analysis produced an adequate isochron fit with a good probability and MSWD near unity. The resultant mineral isochron age for DI-15 is 1330 ± 360 Ma. The very large uncertainty comes from the larger uncertainties associated with the points and the narrow spread of the data. This plot does not include three mineral fractions and means that this plot from DI-15 is not very good for defining the age. Evidently some open-system behavior characterizes Nd isotopes limiting the variability between the mineral phases. However, the “age” calculated and the initial $^{143}\text{Nd}/^{144}\text{Nd}$ is essentially identical to DI-13.

Figure 18 shows the $^{147}\text{Sm}/^{144}\text{Nd}$ versus $^{143}\text{Nd}/^{144}\text{Nd}$ diagram for the seven magnetites, three from the granophyre and four from the diabase.

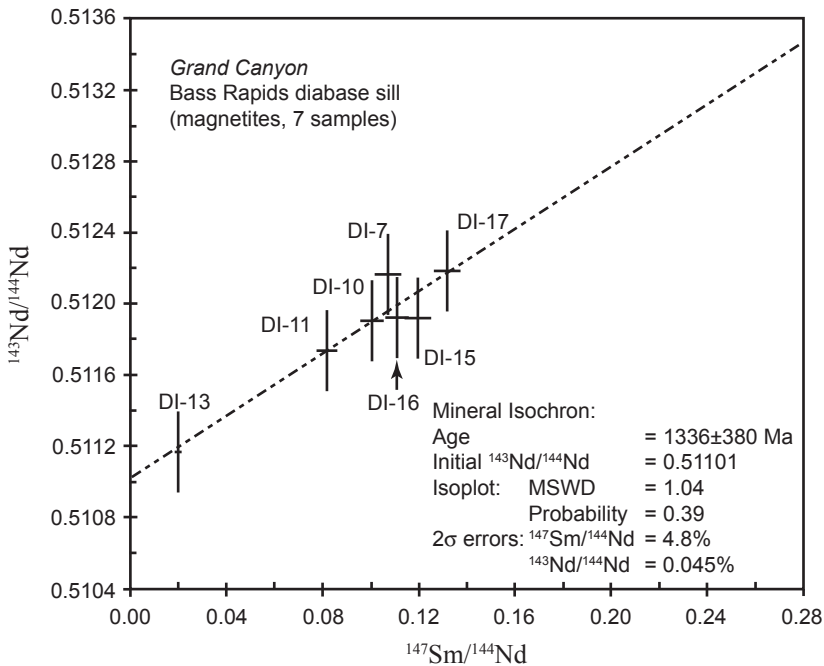


Figure 18. Sm-Nd magnetite mineral isochron for the Bass Rapids diabase sill.

The diagram shows moderate spread among the seven data points. The regression analysis produced an adequate isochron fit with lower probability and MSWD near unity. The resultant mineral isochron “age” for the magnetites is 1336 ± 380 Ma. The plot in many ways resembles the minerals of DI-15 (Figure 17).

7.4 Pb-Pb Data

Figure 19 shows $^{206}\text{Pb}/^{204}\text{Pb}$ plotted against $^{207}\text{Pb}/^{204}\text{Pb}$ for the whole-rock samples from the Bass Rapids diabase sill, based on the data in Table 6. All eleven whole-rock samples were used in the regression analysis and yielded an isochron fit with an “age” of 1250 ± 130 Ma, with a good probability and MSWD near unity. The relatively large 2σ uncertainty in the resultant age is primarily due to the size of the 2σ errors in the data points represented by the ellipses on the diagram.

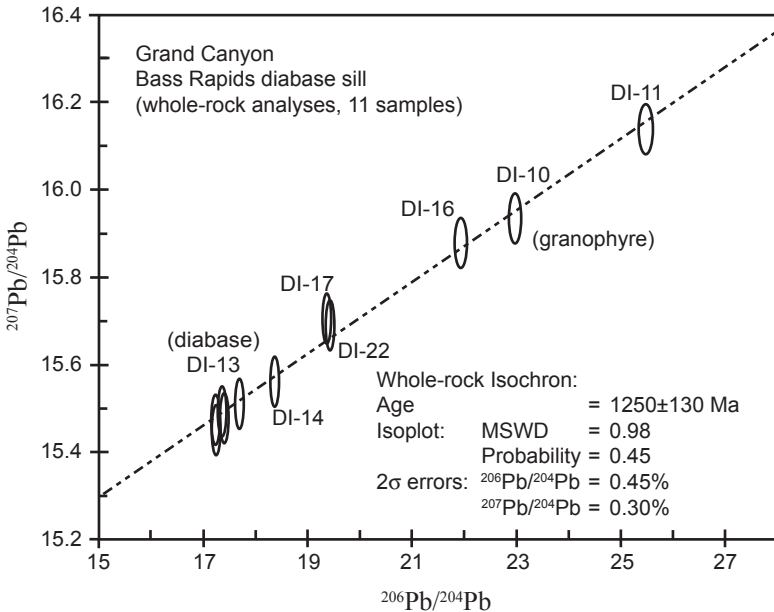


Figure 19. $^{206}\text{Pb}/^{204}\text{Pb}$ versus $^{207}\text{Pb}/^{204}\text{Pb}$ diagram for the Bass Rapids diabase sill, using all eleven whole-rock samples in the isochron and age calculations. The error ellipses represent the 2σ uncertainties.

On the other hand, the three granophyre samples (DI-10, DI-11, and DI-16) give a greater spread to the data which otherwise yields good regression statistics for the isochron.

Figures 20, 21, and 22 show $^{206}\text{Pb}/^{204}\text{Pb}$ plotted against $^{207}\text{Pb}/^{204}\text{Pb}$ for the various minerals, based on the data in Tables 7, 8, and 9 respectively. These three figures are plotted at the same scale as the Pb-Pb whole-rock data (Figure 19). Minerals of DI-13 and DI-15 are shown in Figures 20 and 21. These data are tightly grouped, showing that U is not strongly partitioned between the mineral phases within a single rock. *Isoplot* [Ludwig, 2001] shows no significant Pb-Pb age information can be derived from these seven and ten data points respectively. These mineral data do not define good isochrons, but these minerals do plot along the whole-rock Pb-Pb isochron that is included in both Figures 20 and 21 for reference. Five magnetites and one ilmenite appear to define an

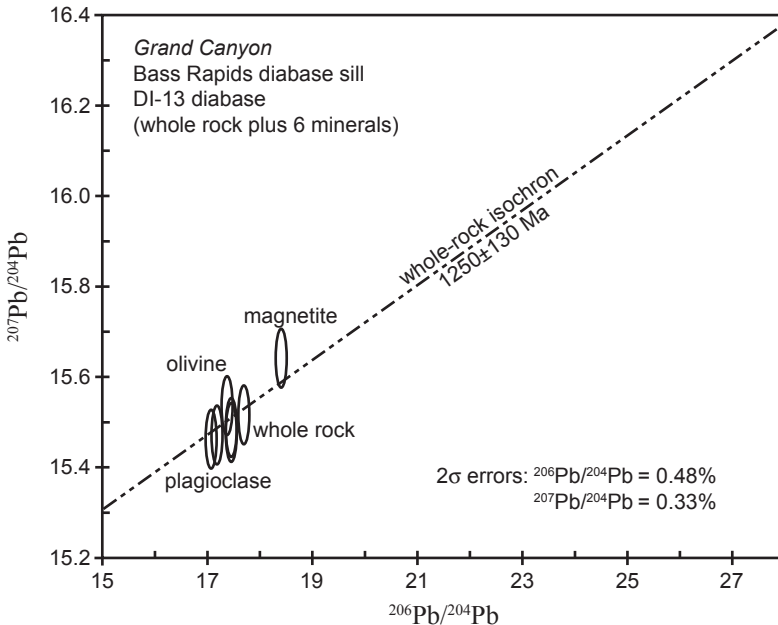


Figure 20. $^{206}\text{Pb}/^{204}\text{Pb}$ versus $^{207}\text{Pb}/^{204}\text{Pb}$ diagram for six mineral fractions from diabase sample DI-13 (plus the whole rock) from the Bass Rapids diabase sill. The error ellipses represent the 2σ uncertainties, and the Pb-Pb whole-rock isochron of Figure 19 is shown for comparison.

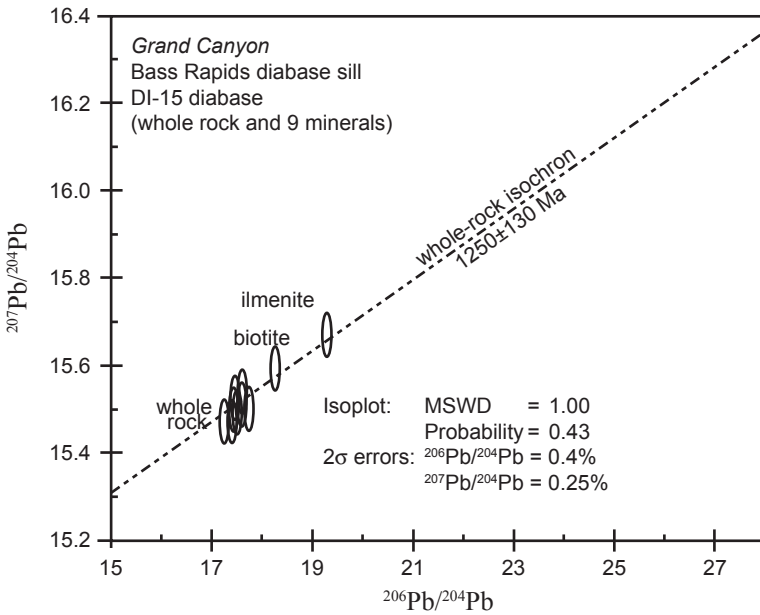


Figure 21. $^{206}\text{Pb}/^{204}\text{Pb}$ versus $^{207}\text{Pb}/^{204}\text{Pb}$ diagram for nine mineral fractions from diabase sample DI-15 (plus the whole rock) from the Bass Rapids diabase sill. The error ellipses represent the 2σ uncertainties, and the Pb-Pb whole-rock isochron of Figure 19 is shown for comparison.

adequate isochron in Figure 22. Two magnetites from the upper contact of the granophyre (DI-10 and DI-11) plot significantly above the line in Figure 22, suggesting Pb contamination from the overlying wall-rock (Figure 5). The lesson to be learned is that the Pb-Pb mineral isochron data is generally concordant with the Pb-Pb whole-rock isochron data.

8. Discussion

8.1 Nature of the Linear Isotope Plots

Isochron plots for the Beartooth amphibolite and Bass Rapids diabase sill reveal extraordinary linearity within the ^{40}K - ^{40}Ar , ^{87}Rb - ^{87}Sr , ^{147}Sm - ^{143}Nd , and ^{207}Pb - ^{206}Pb - ^{204}Pb radioisotope systems. Three mineral isochrons (Rb-Sr, Sm-Nd, and Pb-Pb) are well defined within the Beartooth amphibolite. For Bass Rapids diabase sill, each of the

four radioisotope pairs produced an eleven-point, whole-rock plot. The five Bass Rapids diabase sill whole-rock data plots (Figures 9, 10, 11, 15, and 19) contain 55 data points with 52 points following linear trends. Remarkably, only three of the whole-rock data points plotted significantly off the linear trends. These three data points plotting significantly off the line in Figure 15 are easily explained by the granophyre's assimilation of Nd due to contamination from the adjoining hornfels just above the sill (Figure 5). Certain hydrothermal conditions have been shown to cause REE mobility in rhyolite and granite [Poitrasson *et al.*, 1995], the Nd isotopes being perturbed during hydrothermal alteration. That such hydrothermal alteration of the granophyre in the sill has occurred during contact metamorphism with the overlying shale is evidenced by plagioclase altered to sericite and biotite altered to chlorite. If we allow the magnetite of granophyre samples DI-10,

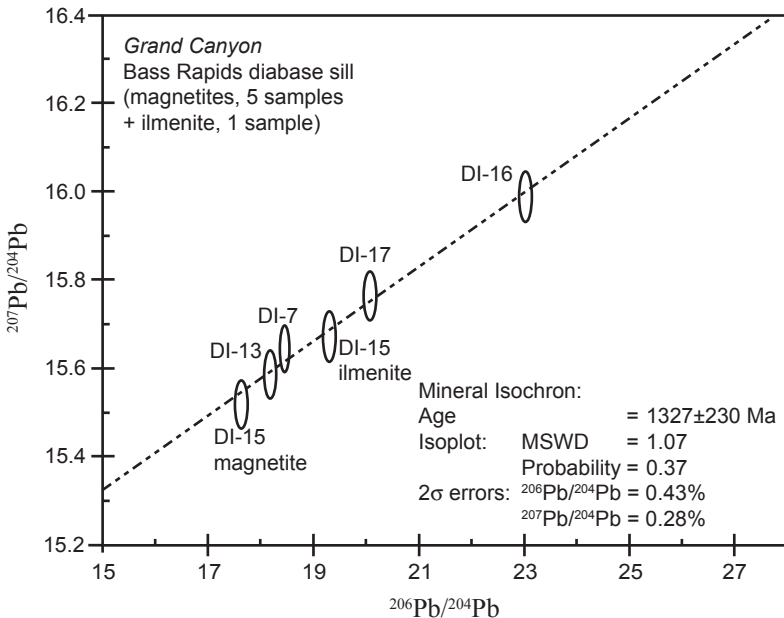


Figure 22. $^{206}\text{Pb}/^{204}\text{Pb}$ versus $^{207}\text{Pb}/^{204}\text{Pb}$ diagram for six magnetite mineral fractions from the Bass Rapids diabase sill. The error ellipses represent the 2σ uncertainties. Two magnetite samples from the granophyre (DI-10 and DI-11) plot above the line and are not shown.

DI-11 and DI-16 to be a proxy for the altered granophyre whole rock, all 55 data points representing whole rocks lie on linear trends.

Some creationists may want to consider the possibility that the remarkably linear isotope ratios within the diabase and granophyre were derived, not by radioisotope decay, but by mixing of two different magmas. Such a model has been proposed by *Giem* [1997], and discussed by *Austin and Snelling* [1998] and *Snelling et al.* [2003]. We might suppose the sill at Bass Rapids was formed from a granophyre magma (higher K, Ar, Rb, Sm, Nd, and U) combined with different proportions of a diabase magma (lower K, Ar, Rb, Sm, Nd, and U). The mixing model supposes these two magmas, and their various magma mixtures, were never in an isotopically homogeneous condition. Isotopes from these two magma types may then have formed the mixing lines in Figures 9, 10, 11, 15, and 19 without radioisotope decay within the rocks. As pointed out by *Austin* [2000], mineral isochron plots provide the data critical for testing the magma mixing model. Mineral phases within any single rock should be homogeneous, because the mixing model supposes rocks crystallized from large, locally mixed, batches of melt, and because, after crystallization, radioisotope decay is assumed to have been minor. For the Bass Rapids diabase sill, however, radioisotopes differ significantly between mineral phases within diabase samples DI-13 and DI-15. Thus, significant radioisotope decay, not mixing, is the favored explanation of the extraordinary linearity. Furthermore, the petrographic and geochemical data from the Bass Rapids sill argues that “unmixing” has occurred (chemical and gravitational segregation from an initially homogeneous, molten condition). The best explanation is exactly opposite the mixing model.

Potassium-40-⁴⁰Ar, ⁸⁷Rb-⁸⁷Sr, ¹⁴⁷Sm-¹⁴³Nd, and ²⁰⁷Pb-²⁰⁶Pb-²⁰⁴Pb radioisotope data provide strong evidence that the Bass Rapids diabase sill was intruded while in an isotopically mixed, homogeneous condition. Initially, the sill was chemically and isotopically homogeneous when the basaltic magma was intruded rapidly into the Hakatai Shale. The word “homogeneous” allows for less than 1% initial variation in ⁸⁷Sr/⁸⁶Sr within the cogenetic suite of whole-rocks (Figure 11), and allows for less than 0.2% initial variation in ⁸⁷Sr/⁸⁶Sr among the minerals within

a single rock (Figure 13). The subsequent mineralogical segregation within the sill was produced by flow differentiation and gravitational settling, resulting in olivine diabase overlain by granophyre. At that time of intrusion the different parts of the newly formed sill had the same Ar, Sr, Nd, and Pb isotopic ratios. The words “the same . . . isotopic ratios” allows for small variation in the daughter isotope ratios as specified by the isochron plots, and, especially, the MSWD analysis. This must be, and is conventionally by definition, the agreed initial condition in order for radioisotope dating of the diabase to be achievable.

8.2 Summary of Isochron Discordance

What then is the finding concerning radioisotopes within minerals of the Beartooth amphibolite sample? What then can be said about the *present* isotopic ratios within whole rocks and minerals of the Bass Rapids sill? Do parent-daughter radioisotope ratios produce a consistent picture of the “age” of the amphibolite metamorphism and intrusion of the sill respectively? A robust Rb-Sr mineral isochron plot (Figure 12) appears to constrain the “age” of the diabase sill to 1060 ± 24 Ma (2σ error). That is the currently accepted age of this Grand Canyon diabase sill according to *Elston and McKee* [1982] and *Larson et al.* [1994] when the diabase sill was isotopically homogeneous with respect to Sr. However, the Sm-Nd mineral isochron plot from DI-13 (Figure 16) is strongly linear giving the “age” for initial homogeneous Nd as 1379 ± 140 Ma (2σ error). Although the uncertainty associated with this Sm-Nd mineral isochron is larger, its “age” is clearly discordant with Rb-Sr. How could the suite of minerals in sample DI-13 have Nd isotopes homogenized at 1379 ± 140 Ma (Figure 16) but not have Nd rehomogenized within the minerals by the event that thoroughly homogenized the Sr isotopes within the minerals of DI-13 at 1060 ± 24 Ma (Figure 12)?

The Pb-Pb whole-rock isochron plot (Figure 19) gives the “age” for initial homogeneous Pb as 1250 ± 130 Ma (2σ error), again discordant with Rb-Sr. How could the suite of whole-rocks within the sill have Pb isotopes homogenized at 1250 ± 130 Ma (Figure 19) but not have Pb rehomogenized within the rocks by the event that thoroughly

homogenized the Sr isotopes at 1060 ± 24 Ma (Figure 12)? Both of these “ages” are discordant with the K-Ar whole-rock isochron age (Figure 9) of 841.5 ± 164 Ma assuming no initial ^{40}Ar . Which of these is the true “age” of the initial isotopic mixing? No internally consistent “age” emerges from these data.

These discordant isochron dates for the Beartooth amphibolite and the Bass Rapids diabase sill are not unique. Indeed, *Austin* [2000] has already documented that, when the mineral isochron method is applied as a test of the assumptions of radioisotope dating, discordances inevitably result. According to *Austin* [2000] four categories of discordance are found in cogenetic suites of rocks—

- (1) two or more discordant whole-rock isochron ages,
- (2) a whole-rock isochron age older than the associated mineral isochron ages,
- (3) two or more discordant mineral isochrons from the same rock, and
- (4) a whole-rock isochron age younger than the associated mineral isochron ages.

Our radioisotope data from the Beartooth amphibolite and Bass Rapids diabase sill exhibit all four categories of isochron discordance. Thus the assumptions of radioisotope dating must be questioned.

8.3 Similarity to the Great Dyke of Zimbabwe

The Great Dyke of the Zimbabwe craton in southeast Africa is a 550 km long layered mafic and ultramafic intrusion 3 to 11 km wide. According to *Oberthür et al.* [2002], five complexes within the Great Dyke are each composed of a lower ultramafic sequence (dunites, harzburgites, olivine bronzitites and pyroxenites) overlain by an upper mafic sequence (plagioclase-rich rocks such as norites, gabbronorites and olivine gabbros). The variation in chemistry and mineralogy of the Great Dyke is particularly suitable to Rb-Sr dating, similar to the diabase to granophyre transition within the Bass Rapids sill of Grand Canyon. *Davies et al.* [1970] reported an eight-point Rb-Sr whole-rock isochron age from the Great Dyke of 2477 ± 90 Ma with initial $^{87}\text{Sr}/^{86}\text{Sr}$ of 0.7024 ± 0.0008 . *Hamilton* [1977] very precisely reconfirmed this

age and initial Sr ratio by plotting a nine-point Rb-Sr whole-rock and mineral isochron (five whole rocks and four mineral separates) of 2455 ± 16 Ma and initial $^{87}\text{Sr}/^{86}\text{Sr}$ of 0.70261 ± 0.00004 . Both of the above ages and initial Sr ratios were again reconfirmed by *Mukasa et al.* [1998] using the core from a single drill-hole into the Great Dyke yielding an 11-point whole-rock and mineral isochron of 2467 ± 85 Ma and initial $^{87}\text{Sr}/^{86}\text{Sr}$ of 0.7026 ± 0.0004 . (All three ages are calculated using λ for $^{87}\text{Rb} = 1.42 \times 10^{-11}$ per year, and errors being 2σ only from the analytical equipment.) The robustness of the Rb-Sr data appears to restrict the age of the Great Dyke to 2455 ± 16 Ma with an initial $^{87}\text{Sr}/^{86}\text{Sr}$ of 0.70260 ± 0.00005 .

Although the 2455 ± 16 Ma Rb-Sr isochron age of the Great Dyke has been widely accepted, recent Sm-Nd, Pb-Pb, and U-Pb data indicate the intrusion is ≈ 120 Ma older than indicated by Rb-Sr. Recently, *Mukasa et al.* [1998] reported an age of 2586 ± 16 Ma (Sm-Nd whole-rock isochron), 2596 ± 14 Ma (Pb-Pb mineral and whole-rock isochron), and 2587 ± 8 Ma (U-Pb rutile). Also recently, numerous reported U-Pb zircon ages [summarized by *Oberthür et al.*, 2002] are concordant with the Great Dyke Sm-Nd and Pb-Pb isochrons. These new data are now widely regarded as having discredited the once generally accepted Rb-Sr isochron age of Great Dyke [*Oberthür et al.*, 2002]. The acceptable “age” of intrusion of Great Dyke is no longer 2455 ± 16 Ma (Rb-Sr whole-rock and mineral isochron), but 2586 ± 16 Ma (Sm-Nd whole-rock isochron), 2587 ± 8 Ma (U-Pb mineral concordia), or 2596 ± 14 Ma (Pb-Pb mineral and whole-rock isochrons), the latter three “ages” being concordant.

Discordant isochron ages were obtained also on the Stuart dyke swarm (Late Proterozoic of south-central Australia) and the Uruguayan dike swarm (Precambrian of Uruguay). The Stuart dyke swarm gave discordant mineral isochron ages of 1076 ± 33 Ma (Sm-Nd mineral isochron) and 897 ± 9 Ma (Rb-Sr mineral isochron with biotite), according to *Zhao and McCulloch* [1993]. The Uruguayan dike swarm yielded a discordant date of 1766 ± 124 (Rb-Sr isochron for fifteen whole rocks) and 1366 ± 18 Ma (Rb-Sr mineral isochron including biotite), according to *Teixeira et al.* [1999].

8.4 Explanations of Discordance

Five possible explanations of the discordant isotope data need to be considered. Here we seek to discover the possible explanations for isochron discordance and evaluate whether the evidence supports such explanation.

8.4.1 Mineral Inheritance with Magma Contamination

The first explanation to consider is the possibility that the Rb-Sr system is telling us the correct age, and the significantly older Pb-Pb and Sm-Nd systems are giving incorrect or spurious ages. We need an elaborate explanation giving reasons why the Sm-Nd and Pb-Pb systems were not homogeneous isotopically with respect to $^{143}\text{Nd}/^{144}\text{Nd}$ and Pb isotopes. *Mukasa et al.* [1998] and *Oberthür et al.* [2002] entertained the possibility that crustal contamination of rising magma in the Great Dyke could create an isotope mixing condition causing false Sm-Nd and Pb-Pb whole-rock isochrons. These authors noted that a high Sr (and low Nd and Pb) magma could be contaminated with smaller amounts of crustal Sr, Pb, and Nd, not significantly affecting the Rb-Sr whole-rock isochron, but causing significant mixing lines on the Pb-Pb and Sm-Nd whole-rock plots, yielding false Pb-Pb and Sm-Nd whole-rock ages. Two explanations can be offered:

- (1) the contaminants were in the liquid phase of the magma, and
- (2) the contaminants were within an included mineral phase or phases within the magma.

The first proposal does not offer an explanation of concordance between Sm-Nd and Pb-Pb whole-rock and mineral isochrons, because the minerals must generate the same false isochron as the suite of whole rocks by some unknown process. Therefore, researchers like *Mukasa et al.* [1998] and *Oberthür et al.* [2002] have entertained the second possibility (that is, the contaminant resided within a mineral phase within the original magma). These researchers, however, have not defended the proposal.

In order to explain the zircon U-Pb data collected by *Oberthür et al.* [2002] for the Great Dyke (and presumably the titanite Pb data for the Beartooth amphibolite), zircon crystals (and presumably titanite in

Beartooth amphibolite) were crystals within the magma at the time of intrusion. We might suppose the zircons were assimilated from the wall rocks that have a much older age. Thus, rocks and cogenetic suites of rocks would not be homogenized isotopically in the beginning. They either acquire contaminants from deep magma chambers and/or from interaction with wall rock within transport conduits. Magmas on the small scale of rocks to the larger scale of extensive formations would either retain or acquire clumps of high and low isotope abundance ratios.

After considering the explanation only briefly, *Mukasa et al.* [1998] and *Oberthür et al.* [2002] dismiss the possibility of mineral inheritance and accompanying magma contamination as an explanation for discordant isochrons in the Great Dyke. These authors report concordant U-Pb concordia and Pb-Pb isochron ages for three mineral phases within the Great Dyke (zircon, rutile, and baddeleyite). Unusually high Th/U ratios in zircon within the Great Dyke argue that zircon is the product of very late stage magmatic crystallization as would occur within a dike [*Oberthür et al.*, 2002]. Zircon chemistry is atypical of most other igneous rocks, including gabbros, disputing the notion that zircon in the Great Dyke is an inherited mineral component.

Within the Beartooth amphibolite and the Bass Rapids diabase sill, major-abundance mineral phases (not just minor-abundance mineral phases) define the Sm-Nd mineral isochrons (Figures 7, 16, and 17). Plagioclase, hornblende and biotite, the main minerals composing the metamorphic fabric of the Beartooth amphibolite, define the Sm-Nd mineral isochron (Figure 7). Plagioclase, hornblende, and biotite must reflect the metamorphic event, not imagined component minerals resistant to metamorphism retained from the protolith. Plagioclase and clinopyroxene, the main minerals composing the Bass Rapids diabase sill, define the Sm-Nd isochron (Figure 16 and 17). Plagioclase and clinopyroxene (along with several other mineral phases) must have been part of the molten magma in order for the mechanical process of sill intrusion to occur. Therefore, plagioclase and clinopyroxene were not inherited mineral phases in the diabase. Furthermore, the concordant Sm-Nd magnetite mineral isochron within the diabase (Figure 18)

indicates that magnetite is not an inherited mineral phase. We can reject the mineral inheritance and magma contamination model for discordant isochron ages in Beartooth amphibolite, Bass Rapids diabase sill, and the Great Dyke.

8.4.2 Slow Cooling

A second explanation for discordant isochrons is the possibility that the different isochron ages can be explained by the minerals cooling extremely slowly to form rocks over hundreds of millions of years. In this view it is impossible to read a single age of amphibolite metamorphism supposing it to be an event. It would also be impossible to discern the age of intrusion and cooling of diabase within a sill as an event. We can think of the slow cooling model as an explanation for discordant mineral isochrons (category three discordance). Also, slow cooling could be offered as an explanation where the mineral isochron of one radioisotope pair is younger than the whole-rock isochron of another radioisotope pair (category two discordance). Proterozoic metamorphic basement rocks of southern Mexico yielded a Sm-Nd whole-rock isochron age of 1440 Ma interpreted as the time of original formation of the continental crust [*Weber and Köhler, 1999*]. Younger U-Pb zircon ages and various mineral isochrons (including a biotite plus whole-rock Rb-Sr isochron) are interpreted as documenting a cooling history extending over 500 Ma [*Weber and Köhler, 1999*].

The proposal of slow cooling does not offer an explanation for discordant whole-rock isochrons (category one discordance) or mineral isochron ages older than associated whole-rock isochron ages (category four discordance). Thus, slow cooling can be rejected as a proposal for category four discordance in the Beartooth amphibolite, and category one and four discordances in the Bass Rapids diabase sill. *Mukasa et al.* [1998] rejected slow cooling as an explanation for the discordant isochron ages in the Great Dyke.

The explanation of slow cooling also leads to a faulty explanation of the geologic context of the Bass Rapids diabase sill. The diabase sill was intruded into much cooler sedimentary rocks (the Hakatai Shale), and the physics of conductivity of heat through solids causes us to question how a 91 m thick magma sill was able to retain molten

minerals within much cooler sediments for hundreds of millions of years [see discussion by *Harrison and McDougall*, 1980]. Thus, in specific details the slow cooling model lacks convincing argument and direct application, especially to the Bass Rapids diabase sill.

8.4.3 Post-Magmatic Loss of Radiogenic Sr

A third possible explanation is that discordant ages are caused by a violation of the closed system assumption of radioisotope dating. If we accept the Pb-Pb and Sm-Nd whole rock and mineral isochrons as true ages, then the Rb-Sr isochrons would be interpreted as significantly altered with a specific bias to give significantly younger but spurious ages. We need to imagine some type of Sr loss process that removed significant ^{87}Sr and/or added significant ^{87}Rb over geologic time. Less likely, but also making Rb-Sr ages much younger, would be addition of Rb, a process not considered further here. Because solid-state diffusion is unlikely through crystalline rocks, a fluid-based Sr-loss process might be imagined resembling a hydrothermal condition [*Mukasa et al.*, 1998]. This Sr-loss process must occur at low temperature because Ar closure evidence within Cardenas Basalt and associated dikes and sills of Grand Canyon indicates temperatures have not exceeded ~ 250 to 300°C after magma emplacement and crystallization [*Larson et al.*, 1994]. Because biotite is the significant mineral determining the Rb-Sr mineral isochrons in the Beartooth amphibolite and the Bass Rapids diabase sill, biotite's closure temperature relative to Sr loss is important. A closure temperature of $\sim 320^\circ\text{C}$ is usually assumed [*Harrison and McDougall*, 1980; *Weber and Köhler*, 1999].

Rubidium-Sr whole-rock isochrons for the Uruguayan dike swarm are significantly older than the Rb-Sr biotite mineral isochron [*Teixeira et al.*, 1999]. According to *Teixeira et al.* [1999], the Rb-Sr mineral data from the Uruguayan dike swarm show significant scatter from the line, a property thought to be diagnostic of post-magmatic Sr isotope disruption. Also diagnostic of post-magmatic Sr disruption in the Rb-Sr mineral isochron, according to *Teixeira et al.* [1999], is *higher* initial $^{87}\text{Sr}/^{86}\text{Sr}$ than that with the associated Rb-Sr whole-rock isochron.

The Beartooth amphibolite Rb-Sr mineral data show very good linearity (Figure 6), and do not possess scatter suggesting the Sr

disruption process (low scatter indicated by the high probability value in Figure 6). Higher initial $^{87}\text{Sr}/^{86}\text{Sr}$ does occur in the Beartooth Rb-Sr mineral isochron (0.7044 in Figure 6) than the associated Rb-Sr whole-rock isochron (0.7022 in Figure 3), a possible indication of alteration. Because the mineral composition and texture of the sample of Beartooth andesitic amphibolite resembles the probable precursor andesite, post-magmatic hydrothermal alteration at $\sim 300^\circ\text{C}$ is not indicated [Mueller *et al.*, 1983]. The geochemical evidence, especially the abundance of REEs, also, points to isochemical metamorphism of the probable andesite precursor, not significant hydrothermal alteration [Mueller *et al.*, 1983]. Thus, it is doubtful if post-magmatic Sr loss can explain the Rb-Sr mineral isochron in the Beartooth amphibolite.

The Bass Rapids diabase sill Rb-Sr mineral isochrons (Figures 12 and 13) display excellent linearity, not suggestive of post-magmatic Sr disruption. Lower initial $^{87}\text{Sr}/^{86}\text{Sr}$ occur in the diabase sill Rb-Sr mineral isochrons (0.7030 and 0.7039 in Figures 12 and 13) than the associated Rb-Sr whole-rock isochron (0.7043 in Figure 11), another significant problem for post-magmatic Sr loss. Strontium remains in high abundance relative to geochemically similar Ca (Table 2) indicating conservation of Sr, not loss of Sr. Conservation of Sr is evident even though petrographic evidence indicates some alteration of plagioclase to sericite and some alteration of biotite to chlorite. The geochemical evidence for open-system behavior is limited to the Nd in the Sm-Nd radioisotope system in the granophyre whole-rock samples (perturbed by contamination from the overlying hornfels wall rock), and possibly to a few mineral species that lie off the trend lines established strongly by the majority of the other minerals. The general closed-system assumption for the Bass Rapids diabase sill Rb-Sr system is not unreasonable.

The post-magmatic Sr loss (and/or Rb gain) explanation for the Rb-Sr mineral isochron for the Bass Rapids diabase sill has one last extremely significant problem. Post-magmatic Sr loss (and/or Rb gain) could, possibly, explain the robust Rb-Sr mineral isochrons, but how does it explain the *concordant* Rb-Sr whole rock isochron? We need to explain why Figures 12 and 13 compare so well with Figure 11. As

Mukasa et al. [1998] admitted for the concordant Rb-Sr mineral and whole-rock isochrons for the Great Dyke, "...there is no good reason why both mineral and whole-rock samples would be altered to give the same erroneous age." Not only must the Rb-Sr whole rocks of the Bass Rapids diabase sill be depleted of significant ^{87}Sr , but the Cardenas Basalt and other associated dikes and sills must be depleted as well. As pointed out by *Larson et al.* [1994] a regionally extensive Rb-Sr whole-rock pattern exists indicating an "age" of 1103 ± 66 Ma. To dispose of ^{87}Sr on such a large scale would require an extraordinary hydrothermal alteration system. Thus, post-magmatic Sr loss is an extremely unlikely explanation for the Rb-Sr mineral and whole-rock isochrons in the Bass Rapids diabase sill.

8.4.4 Uncertainties in Determinations of Decay Constants

As already argued, corroborative evidence indicates that both the amphibolite and the diabase sill initially had a homogeneous mixture of Ar, Sr, Nd, and Pb isotopes. Thus the assumption about the initial conditions for the sill and these radioisotope systems must be valid. Also, a very good case can be made for the general closed-system behavior for these rocks with respect to most of the radioisotope pairs. Therefore, could the differences in the calculated "ages" above be caused by errors in determining the "constants" of radioisotope decay? According to *Steiger and Jäger* [1977], U decay constants are measured reproducibly with great precision to four significant figures. Therefore, no significant decay-constant error occurs with Pb-Pb isochrons. *Steiger and Jäger* [1977] recommended the decay constant for ^{87}Rb of 1.42×10^{-11} per year that is in wide use by the geochronologic community, but offered no uncertainty associated with the decay constant. *Begemann et al.* [2001] recommend λ $^{87}\text{Rb} = 1.406 \pm 0.008 \times 10^{-11}$ per year, whereas *and Zaitsev* [2002] suggested λ for $^{87}\text{Rb} = 1.396 \pm 0.006 \times 10^{-11}$ per year. However, this small change would not close the discordance between the Rb-Sr and either the Pb-Pb or Sm-Nd systems in Beartooth amphibolite or Bass Rapids diabase. According to *Begemann et al.* [2001], researchers generally agree that the decay constant for ^{147}Sm has been determined to three significant figures (6.54×10^{-12}).

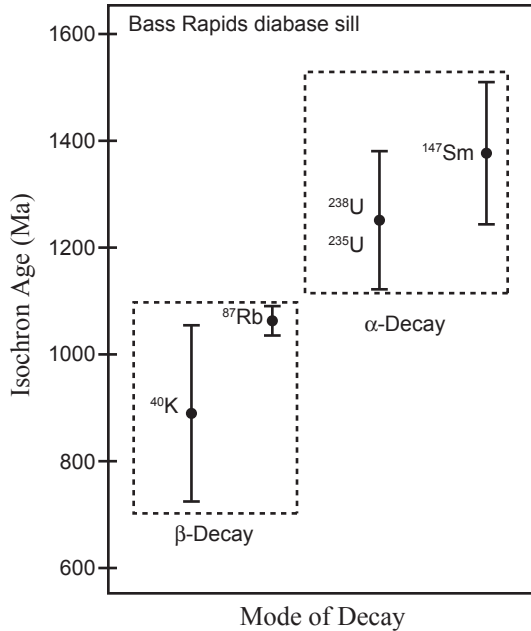


Figure 23. Isochron age versus mode of decay for the four radioisotope systems within Bass Rapids diabase sill. Alpha-emitters give older “ages” than β -emitters.

8.4.5 Have Decay Constants Always been Constant?

Our data indicate that the α -emitters (^{238}U , ^{235}U , and ^{147}Sm) have yielded older ages than the β -emitters (^{87}Rb and ^{40}K) when used to date the same geologic event, that is, the metamorphism of andesite to produce the Beartooth amphibolite or the intrusion of the Bass Rapids diabase sill. Ages for the Bass Rapids diabase sill are shown in Figure 23. A logical explanation of these data is that the radioisotope decay of the various parent isotopes has not always proceeded at the rates described by modern decay “constants,” the discordances being due to the different parent radioisotopes decaying at different rates over the *same* time periods since the metamorphism of the andesite and the intrusion of the diabase sill. These data are consistent with the notion that the decay of these parent radioisotopes was accelerated by different

amounts. Thus, our data indicate that α -decay was accelerated more than β -decay at some time or times in the past.

Do our data suggest a correlation between the present radioactive decay constants for these α - and β -emitters and the “ages” they have yielded for these same geologic events? Of the α -emitters, ^{147}Sm has the smallest decay constant (and thus the longest half-life), and it yielded the oldest “age” for the diabase sill, a Sm-Nd mineral isochron “age” of 1379 ± 140 Ma (Figure 16), compared to the Pb-Pb whole-rock isochron “age” of 1250 ± 130 Ma (Figure 19). Although error bars on “ages” for these two α -emitters overlap for the diabase sill, error bars for the Beartooth mineral isochrons more strongly indicate older “ages” for Sm-Nd than for Pb-Pb (compare Figures 7 and 8). Similarly, of the β -emitters, ^{87}Rb has the smaller decay constant (and thus the longer half-life) and it yielded the older “ages” for the diabase sill, a whole-rock isochron “age” of 1055 ± 46 Ma (Figure 11) and a mineral isochron “age” of 1060 ± 24 Ma (Figure 12), compared to the K-Ar whole-rock isochron “age” of 841.5 ± 164 Ma (Figure 9). We can say our data are consistent with the possibility that the longer the half-life of the α - or β -emitter the more its decay has been accelerated, relative to the other α - or β -emitters, at some time or times in the past.

Other explanations for the same discordant isochron data can be offered. It is even possible to use the same data to argue that there is *no correlation* between the present radioactive decay constants and the “ages” they have yielded for the same geologic events. Thus, for the α -emitters, the diabase mineral isochron age of 1379 ± 140 Ma (Figure 16) can be regarded statistically as concordant with the Pb-Pb whole-rock isochron “age” of 1250 ± 130 Ma (Figure 19) because the assigned errors overlap (Figure 23). The notion of concordance between the α -emitters is supported by concordant ages, as stated above, for the Great Dyke. These concordant α -emitter ages for the Great Dyke are 2586 ± 16 Ma (Sm-Nd whole-rock isochron), 2587 ± 8 Ma (U-Pb mineral concordia), and 2596 ± 14 Ma (Pb-Pb mineral and whole-rock isochrons).

The important observation derived from Beartooth andesitic amphibolite and the Bass Rapids diabase sill, verified by study of the

Great Dyke, is that α -emitters give older ages than β -emitters when applied to the same rocks. It is recommended that further similar studies of suitable rock units be undertaken to extend and confirm these findings. Further research on Precambrian sills and dikes, especially using Sm-Nd and Pb-Pb, should be conducted.

9. Conclusions

The distributions of parent and daughter radioisotopes in the Archean Beartooth amphibolite and in the middle Proterozoic Bass Rapids diabase sill reveal a significant problem with the assumptions of conventional radioisotope dating. Even though several lines of evidence confirm that the daughter isotopes were homogeneously mixed when the andesite was metamorphosed to amphibolite and the basaltic magma was intruded initially to form the sill, the four analyzed radioisotope systems yield discordant isochron “ages” for these geologic events. Although significant discordance exists between the K-Ar, Rb-Sr, Sm-Nd, and Pb-Pb radioisotope methods, each method appears to yield concordant “ages” internally between whole-rocks and minerals. Internal concordance is best illustrated by the diabase sill Rb-Sr whole-rock and mineral isochron “ages” of 1055 ± 46 Ma and 1060 ± 24 Ma, respectively. Furthermore, only limited evidence exists for open-system behavior. Open-system behavior is indicated by contamination of the whole-rock Sm-Nd radioisotope system in the granophyre at the top of the diabase sill immediately adjacent to the overlying hornfels wall rock. Therefore, it is concluded that it is the constant decay rates assumption of conventional radioisotope dating that is potentially invalid, and thus changing decay rates in the past could account for the demonstrated discordances between the resultant isochron “ages.” Furthermore, our data are consistent with the possibilities that, at some time or times in the past, decay of the α -emitters (^{238}U , ^{235}U , and ^{147}Sm) was accelerated more than decay of the β -emitters (^{87}Rb and ^{40}K). Conventional radioisotope clocks need repair.

Acknowledgments

Andrew A. Snelling contributed significantly to sample collection, data analysis and writing of the manuscript. Without Andrew's significant help and encouragement during a fourteen-year period this research would not have been completed. William A. Hoesch assisted in laboratory analysis, especially mineral separations. Professor Lang Farmer assisted with attention to detail in the isotope analysis. Grand Canyon National Park provided special use permits allowing access to the remote site of the Bass Rapids sill and granting permission to collect rock samples. Private donors provided financial support through the RATE project, and the project preceding RATE, both administrated at the Institute for Creation Research.

References

- Amelin, Y., and A.N. Zaitsev, Precise geochronology of phoscorites and carbonatites: the critical role of U-series disequilibrium in age interpretations, *Geochimica et Cosmochimica Acta*, 66, 2399–2419, 2002.
- Austin, S. A., Mineral isochron method applied as a test of the assumption of radioisotope dating, in *Radioisotopes and the Age of the Earth: A Young-Earth Creationist Research Initiative*, edited by L. Vardiman, A. A. Snelling, and E. F. Chaffin, pp. 95–121, Institute for Creation Research, El Cajon, California and Creation Research Society, St. Joseph, Missouri, 2000.
- Austin, S. A., and A. A. Snelling, Discordant potassium-argon model and isochron “ages” for Cardenas Basalt (Middle Proterozoic) and associated diabase of eastern Grand Canyon, Arizona, in *Proceedings of the Fourth International Conference on Creationism*, edited by R. E. Walsh, pp. 35–51, Creation Science Fellowship, Pittsburgh, Pennsylvania, 1998.
- Babcock, R. S., Precambrian crystalline core, in *Grand Canyon Geology*, edited by S. S. Beus and M. Morales, first edition, pp. 11–28, Oxford University Press, New York, 1990.
- Begemann, F., K. R. Ludwig, G. W. Lugmair, K. Min, L. E. Nyquist, P. J. Patchett, P. R. Renne, C. Y. Shih, I. M. Villa, and R. J. Walker, Call for

- improved set of decay constants for geochronological use, *Geochimica et Cosmochimica Acta*, 65, 111–121, 2001.
- Bhattacharji, S., Scale model experiments on flowage differentiation in sills, in *Ultramafic and Related Rocks*, edited by P.J. Wyllie, pp.69–70, John Wiley & Sons, New York, 1967.
- Bhattacharji, S., and C.H. Smith, Flowage differentiation, *Science*, 145, 150–153, 1964.
- Dalrymple, G.B., $^{40}\text{Ar}/^{36}\text{Ar}$ Analyses of historic lava flows, *Earth and Planetary Science Letters*, 6, 47–55, 1969.
- Dalrymple, G.B., and M. A. Lanphere, *Potassium-Argon Dating: Principles, Techniques and Applications for Geochronology*, W.H. Freeman, San Francisco, 1969.
- Davies, R. D., H. L. Allsopp, A. Erlank, and J. W. I. Manton, Sr isotopic studies on various layered mafic intrusions in Southern Africa, in *Symposium on the Bushveld Igneous Complex and Other Layered Intrusions*, pp. 576–593, Geological Society of South Africa, Special Publication 1, 1970.
- Elston, D.P., Grand Canyon Supergroup, northern Arizona: stratigraphic summary and preliminary paleomagnetic correlations with parts of other North American Proterozoic successions, in *Geologic Evolution of Arizona*, edited by J.P. Jenney and S. J. Reynolds, pp. 259–272, Arizona Geological Society, Tucson, Digest 17, 1989.
- Elston, D.P., and C.S. Grommé, Precambrian polar wandering from Unkar Group and Nankowep Formation, eastern Grand Canyon, Arizona, in *Geology of Northern Arizona*, edited by T.N.V. Karlstrom, J.A. Swann, and R.L. Eastwood, pp.97–117, Geological Society of America, Rocky Mountain Sectional Meeting, Flagstaff, Arizona, 1974.
- Elston, D.P., and E.H. McKee, Age and correlation of the Late Proterozoic Grand Canyon disturbance, northern Arizona, *Geological Society of America Bulletin*, 93, 681–699, 1982.
- Farmer, G.L., D.E. Broxton, R.G. Warren, and W. Pickthorn, Nd, Sr, and O isotopic variations in metaluminous ash-flow tuffs and related volcanic rocks at the Timber Mountain/Oasis Valley Caldera, Complex, SW Nevada: implications for the origin and evolution of large-volume silicic magma bodies, *Contributions to Mineralogy and Petrology*, 109, 53–68, 1991.
- Ford, T.D., W.J. Breed, and J.S. Mitchell, Name and age of the Upper

- Precambrian basalts in the eastern Grand Canyon, *Geological Society of American Bulletin*, 81, 223–226, 1972.
- Giem, P. A. L., *Scientific Theology*, La Sierra University Press, Riverside, California, pp. 144–146, 1997.
- Hamilton, J., Sr isotope and trace element studies of the Great Dyke and Bushveld mafic phase and their relation to early Proterozoic magma genesis in southern Africa, *Journal of Petrology*, 18, 24–52, 1977.
- Harrison, T.M., and I. McDougall, Investigations of an intrusive contact, northwest Nelson, New Zealand—I. Thermal, chronological and isotopic constraints, *Geochimica et Cosmochimica Acta*, 44, 1985–2003, 1980.
- Hendricks, J.D., *Younger Precambrian Basaltic Rocks of the Grand Canyon, Arizona*, Unpublished M. S. Thesis, Northern Arizona University, Flagstaff, 1972.
- Hendricks, J.D., Petrology and chemistry of igneous rocks of Middle Proterozoic Unkar Group, Grand Canyon Supergroup, northern Arizona, in *Geology of the Grand Canyon, Northern Arizona (with Colorado River Guides)*, edited by D.P. Elston, G.H. Billingsley, and R.A. Young, pp. 106–116, American Geophysical Union, Washington, DC, 1989.
- Hendricks, J.D., and I. Lucchitta, Upper Precambrian igneous rocks of the Grand Canyon, Arizona, in *Geology of Northern Arizona*, edited by T.N.V. Karlstrom, J.A. Swann, and R.L. Eastwood, pp. 65–86, Geological Society of America, Rocky Mountain Sectional Meeting, Flagstaff, Arizona, 1974.
- Hendricks, J.D., and G.M. Stevenson, Grand Canyon Supergroup: Unkar Group, in *Grand Canyon Geology*, first edition, edited by S.S. Beus and M. Morales, pp. 29–47, Oxford University Press, New York, 1990.
- Hendricks, J.D., and G.M. Stevenson, Grand Canyon Supergroup: Unkar Group, in *Grand Canyon Geology*, second edition, edited by S.S. Beus and M. Morales, second edition, pp. 39–52, Oxford University Press, New York, 2003.
- Ilg, B.R., K.E. Karlstrom, D.P. Hawkins, and M.L. Williams, Tectonic evolution of Paleoproterozoic rocks in the Grand Canyon: insights into middle-crustal processes, *Geological Society of America Bulletin*, 108, 1149–1166, 1996.
- Karlstrom, K.E., B.R. Ilg, M.L. Williams, D.P. Hawkins, S.A. Bowring,

- and S. J. Seaman, Paleoproterozoic Rocks of the Granite Gorges, in *Grand Canyon Geology*, edited by S. S. Beus and M. Morales, second edition, pp. 9–38, Oxford University Press, New York, 2003.
- Larson, E. E., P. E. Patterson, and F. E. Mutschler, Lithology, chemistry, age and origin of the Proterozoic Cardenas Basalt, Grand Canyon, Arizona, *Precambrian Research*, 65, 255–276, 1994.
- Ludwig, K. R., *Isoplot/Ex (Version 2.49): The Geochronological Toolkit for Microsoft Excel*, University of California Berkeley, Berkeley Geochronology Center, Special Publication No. 1a, 2001.
- Maxson, J. H., *Preliminary Geologic Map of the Grand Canyon and Vicinity, Arizona, Eastern Section*, Grand Canyon Natural History Association, scale 1:62,500, 1967.
- Maxson, J. H., *Preliminary Geologic Map of the Grand Canyon and Vicinity, Arizona, Western Section*, Grand Canyon Natural History Association, scale 1:62,500, 1968.
- McKee, E. H., and D. C. Noble, Rb-Sr Age of the Cardenas Lavas, Grand Canyon, Arizona, *Geology of Northern Arizona*, edited by T. N. V. Karlstrom, G. A. Swann, and R. L. Eastwood, pp. 87–96, Geological Society of America, Rocky Mountain Sectional Meeting, Flagstaff, 1974.
- McKee, E. H., and D. C. Noble, Age of the Cardenas Lavas, Grand Canyon, Arizona, *Geological Society of America Bulletin*, 87, 1188–1190, 1976.
- Mueller, P. A., J. L. Wooden, K. Schulz, and D. R. Bowes, Incompatible-element-rich andesitic amphibolites from the Archean of Montana and Wyoming: evidence for mantle metasomatism, *Geology*, 11, 203–206, 1983.
- Mueller, P. A., W. W. Locke, and J. L. Wooden, A study in contrasts: Archean and Quaternary geology of the Beartooth Highway, Montana and Wyoming, *Rocky Mountain Section of the Geological Society of America, Centennial Field Guide*, vol. 2, pp. 75–78, 1987.
- Mueller, P. A., R. Shuster, M. Graves, J. Wooden, and D. Bowes, Age and composition of a Late Archean magmatic complex, Beartooth Mountains, Montana-Wyoming, Montana, in *Precambrian and Mesozoic Plate Margins, Montana, Idaho and Wyoming*, edited by S. Lewis and R. B. Berg, Montana Bureau of Mines and Geology, Special Publication 96, pp. 23–42, 1988.
- Mueller, P. A., J. L. Wooden, A. P. Nutman, and D. W. Mogk, Early Archean

- crust in the northern Wyoming province: evidence from U-Pb ages of detrital zircons, *Precambrian Research*, 91, 295–307, 1998.
- Mukasa, S. B., A. H. Wilson, and R. W. Carlson, A multielement geochronologic study of the Great Dyke, Zimbabwe: significance of the robust and reset ages, *Earth and Planetary Science Letters*, 164, 353–369, 1998.
- Noble, L. F., Contributions to the geology of the Grand Canyon, Arizona: the geology of the Shinumo Area, *American Journal of Science*, 29, 369–386, 497–528, 1910.
- Noble, L. F., The Shinumo quadrangle, Grand Canyon district, Arizona, *U.S. Geological Survey, Bulletin 549*, 1914.
- Oberthür, T., D. W. Davis, T. G. Blenkinsop, and A. Höhndorf, Precise U-Pb mineral ages, Rb-Sr and Sm-Nd systematics for the Great Dyke, Zimbabwe—constraints on Late Archean events in the Zimbabwe craton and Limpopo belt, *Precambrian Research*, 113, 293–305, 2002.
- Poitrasson, F., C. Pin, and J.-L. Duthou, Hydrothermal remobilization of rare earth elements and its effects on Nd isotopes in rhyolite and granite, *Earth and Planetary Science Letters*, 130, 1–11, 1995.
- Renne, P. R., D. B. Karner, and K. R. Ludwig, Absolute ages aren't exactly, *Science*, 282, 1840–1841, 1998.
- Simkin, T., Flow Differentiation in the picritic sills of North Skye, in *Ultramafic and Related Rocks*, edited by P. J. Wyllie, pp. 64–69, John Wiley & Sons, New York, 1967.
- Snelling, A. A., S. A. Austin, and W. A. Hoesch, Radioisotopes in the diabase sill (Upper Precambrian) at Bass Rapids, Grand Canyon, Arizona: an application and test of the isochron dating method, in *Proceedings of the Fifth International Conference on Creationism*, edited by R. L. Ivey, Jr., pp. 269–284, Creation Science Fellowship, Pittsburgh, Pennsylvania, 2003.
- Steiger, R. H., and E. Jäger, Subcommittee on geochronology: convention on the use of decay constants in geo- and cosmochronology, *Earth and Planetary Science Letters*, 36, 359–362, 1977.
- Teixeira, W., P. R. Renne, G. Bossi, N. Campal, and M. S. D'Agrella Filho, ^{40}Ar - ^{39}Ar and Rb-Sr geochronology of the Uruguayan dike swarm, Rio de la Plata craton and implications for Proterozoic intraplate activity in western Gondwana, *Precambrian Research*, 93, 153–180, 1999.

- Timmons, M. J., K. E. Karlstrom, C. M. Dehler, J. W. Geissman, and M. T. Heizler, Proterozoic multistage (ca. 1.1 and 0.8 Ga) extension recorded in the Grand Canyon Supergroup and establishment of northwest- and north-trending tectonic grains in the southwestern United States, *Geological Society of America Bulletin*, 113, 163–180, 2001.
- Warner, J. L., R. Lee-Berman, and C. H. Simonds, Field and petrologic relations of some Archean rocks near Long Lake, eastern Beartooth Mountains, Montana and Wyoming, in *Precambrian Geology of the Beartooth Mountains, Montana and Wyoming*, edited by P. A. Mueller and J. L. Wooden, pp. 56–68, Montana Bureau of Mines and Geology, Special Publication 84, 1982.
- Weber, B., and H. Köhler, Sm-Nd, Rb-Sr and U-Pb geochronology of a Grenville Terrane in Southern Mexico: origin and geologic history of the Guichicovi Complex, *Precambrian Research*, 96, 245–262, 1999.
- Weil, A. B., J. W. Geissman, M. Heizler, and R. Van der Voo, Paleomagnetism of Middle Proterozoic mafic intrusions and Upper Proterozoic (Nankoweap) redbeds from the lower Grand Canyon Supergroup, Arizona, *Tectonophysics*, 375, 199–220, 2003.
- Wooden, J. L., P. A. Mueller, D. K. Hunt, and D. R. Bowes, Geochemistry and Rb-Sr geochronology of the Archean rocks from the interior of the southeastern Beartooth Mountains, Montana and Wyoming, in *Precambrian Geology of the Beartooth Mountains, Montana and Wyoming*, edited by P. A. Mueller and J. L. Wooden, pp. 45–55, Montana Bureau of Mines and Geology, Special Publication 84, 1982.
- York, D., Least squares fitting of a straight line with correlated errors, *Earth and Planetary Science Letters*, 5, 320–324, 1969.
- Zhao, J., and M. T. McCulloch, Sm-Nd mineral isochron ages of Late Proterozoic dyke swarms in Australia: evidence for two distinctive events of mafic magmatism and crustal extension, *Chemical Geology*, 109, 341–354, 1993.